

Correlations of errors in measurements of CP violation at neutrino factories

John Pinney^{1 *} and Osamu Yasuda^{2 †}

¹*The Daiwa Anglo-Japanese Foundation
Daiwa Securities Kabuto-cho Bldg 9F
1-1-9 Nihonbashi Kayabacho, Chuo-ku, Tokyo 103-0025, Japan*

²*Department of Physics, Tokyo Metropolitan University
Minami-Osawa, Hachioji, Tokyo 192-0397, Japan
(May, 2001)*

Abstract

Using $\Delta\chi^2$ which is defined by the difference of the number of events with the CP phase δ and the hypothetical one with $\delta = 0$, we discuss correlations of errors of the CP phase and other oscillation parameters as well as the matter effect in measurements at neutrino factories. By varying the oscillation parameters and the normalization of the matter effect, we evaluated the data size required to reject a hypothesis with $\delta = 0$ at 3σ CL. The optimum muon energy and the baseline depends on the magnitude of θ_{13} , the background fraction, the uncertainty of the normalization of the matter effect, but in general lie in the ranges $20\text{GeV} \lesssim E_\mu \lesssim 50\text{GeV}$, $1000\text{km} \lesssim L \lesssim 3000\text{km}$. If we assume that the uncertainty of the matter effect is as large as 20% then the optimum values may be modified to $E_\mu \lesssim 10\text{GeV}$, $L \lesssim 1000\text{km}$ due to the strong correlation of δ and the matter effect. We show analytically that sensitivity to CP violation is lost for $E_\mu \ll 10\text{GeV}$ or for $E_\mu \gg 50\text{GeV}$. We also discuss the possibility of measuring CP violation at the upgraded JHF experiment by taking all the error correlations into account, and show that it is possible to demonstrate $\delta \neq 0$ at 3σ CL for $\theta_{13} \gtrsim 3^\circ$.

13.15.+g, 14.60.Pq, 23.40.Bw, 26.65.+t

Typeset using REVTeX

*Email: jpinney@phys.metro-u.ac.jp

†Email: yasuda@phys.metro-u.ac.jp

I. INTRODUCTION

There have been several experiments [1–11] which suggest neutrino oscillations. It has been shown in the two flavor framework that the solar neutrino deficit can be explained by neutrino oscillation with the set of parameters $(\Delta m_{\odot}^2, \sin^2 2\theta_{\odot}) \simeq (\mathcal{O}(10^{-5}\text{eV}^2), \mathcal{O}(10^{-2}))$ (small angle MSW solution), $(\mathcal{O}(10^{-5}\text{eV}^2), \mathcal{O}(1))$ (large angle MSW solution), or $(\mathcal{O}(10^{-10}\text{eV}^2), \mathcal{O}(1))$ (vacuum oscillation solution), and the atmospheric neutrino anomaly can be accounted for by $(\Delta m_{\text{atm}}^2, \sin^2 2\theta_{\text{atm}}) \simeq (10^{-2.5}\text{eV}^2, 1.0)$.

In the three flavor framework there are two independent mass squared differences and it is usually assumed that these two mass differences correspond to Δm_{\odot}^2 and Δm_{atm}^2 . Throughout this paper we will assume three neutrino species which can account for only the solar neutrino deficit and the atmospheric neutrino anomaly¹. Without loss of generality we assume $|\Delta m_{21}^2| < |\Delta m_{32}^2| < |\Delta m_{31}^2|$ where $\Delta m_{ij}^2 \equiv m_i^2 - m_j^2$. The flavor eigenstates are related to the mass eigenstates by $U_{\alpha j}$ ($\alpha = e, \mu, \tau$), where $U_{\alpha j}$ are the elements of the MNS mixing matrix U [12]:

$$\begin{pmatrix} \nu_e \\ \nu_{\mu} \\ \nu_{\tau} \end{pmatrix} = U \begin{pmatrix} \nu_1 \\ \nu_2 \\ \nu_3 \end{pmatrix},$$

$$U \equiv \begin{pmatrix} U_{e1} & U_{e2} & U_{e3} \\ U_{\mu 1} & U_{\mu 2} & U_{\mu 3} \\ U_{\tau 1} & U_{\tau 2} & U_{\tau 3} \end{pmatrix} = \begin{pmatrix} c_{12}c_{13} & s_{12}c_{13} & s_{13}e^{-i\delta} \\ -s_{12}c_{23} - c_{12}s_{23}s_{13}e^{i\delta} & c_{12}c_{23} - s_{12}s_{23}s_{13}e^{i\delta} & s_{23}c_{13} \\ s_{12}s_{23} - c_{12}c_{23}s_{13}e^{i\delta} & -c_{12}s_{23} - s_{12}c_{23}s_{13}e^{i\delta} & c_{23}c_{13} \end{pmatrix}.$$

With the mass hierarchy $|\Delta m_{21}^2| \ll |\Delta m_{32}^2|$ there are two possible mass patterns which are depicted in Fig. 1a and 1b, depending on whether Δm_{32}^2 is positive or negative. If the matter effect is relevant then the sign of Δm_{32}^2 can be determined by distinguishing neutrinos and anti-neutrinos. The Superkamiokande experiment uses water Cherenkov detectors and events of neutrinos and anti-neutrinos are unfortunately indistinguishable, so the sign of Δm_{32}^2 is unknown to date.

It has been shown in the three flavor framework [13–15] of the CHOOZ reactor data [16] and the atmospheric neutrino data implies very small θ_{13} , i.e., $\sin^2 2\theta_{13} < 0.1$ which is essentially the result of the CHOOZ data. When $|\theta_{13}|$ is small, the MNS matrix looks like

$$U \simeq \begin{pmatrix} c_{\odot} & s_{\odot} & \epsilon \\ -s_{\odot}c_{\text{atm}} & c_{\odot}c_{\text{atm}} & s_{\text{atm}} \\ s_{\odot}s_{\text{atm}} & -c_{\odot}s_{\text{atm}} & c_{\text{atm}} \end{pmatrix},$$

where θ_{12} , θ_{23} have been replaced by θ_{\odot} and θ_{atm} , respectively.

Measurements of θ_{13} and even CP phase δ may be possible in the near future projects [17,18]. Neutrino factories [19,20] have been proposed to measure θ_{13} , the sign of Δm_{32}^2 and CP phase δ , and a lot of people have worked out many aspects in detail [20–33].

Since measurement of CP violation is the main motivation for neutrino factories, it is important to examine errors of the CP phase δ taking into consideration all possible sources

¹To explain the LSND anomaly [11] one needs at least four neutrino species.

of uncertainties in the oscillation parameters as well as matter effects. In this paper we discuss correlations of errors of δ and the matter effect, as well as θ_{kl} and Δm_{kl}^2 .² We find that the correlation of δ and the matter effect is strong for ($E_\mu=50$ GeV, $L \simeq 3000$ km), which has been advocated as the best choice, and if the uncertainty of the matter effect is larger than 5 % then baselines shorter than 3000km are advantageous.

There have been works [32,34,35] which advocated the advantage of conventional low energy neutrino beams over neutrino factories with high energy, and there does not seem to be consensus among the community of neutrino physicists about the optimum neutrino energy and the baseline. One of the purposes of this paper is to show that neutrino factories with high or medium muon energy ($20\text{GeV} \lesssim E_\mu \lesssim 50\text{GeV}$) are more advantageous over experiments with low energy ($E_\mu \ll 10\text{GeV}$). We evaluate the statistical significance of possible CP violation in neutrino factory type experiments for a range of the muon energy $0.5\text{GeV} \leq E_\mu \leq 50\text{GeV}$ and the baseline $10\text{km} \leq L \leq 10^4\text{km}$ and we show that the case $E_\mu \lesssim$ a few GeV is always inferior to the option with higher energy. On the other hand, Lipari [36] has shown that long baseline experiments lose the sensitivity for CP violation for extremely high energy. We will show analytically that the two kinds of $\Delta\chi^2$ that we will use, one of which is defined through the difference of $\delta \neq 0$ and $\delta = 0$ and the other of which through T violation, decrease for large muon energy $E_\mu \gg 50\text{GeV}$.

We also analyze the possibility to measure CP violation at the upgraded JHF experiment with 4MW power and a one mega ton detector. We show that measurement of CP violation is possible for a relatively large value of θ_{13} . It is possible mainly because the detector size is so huge.

In section 2 we analyze numerically the effect of the CP phase δ in neutrino factories by introducing $\Delta\chi^2$ which is defined as the square of the difference of the number of events with $\delta \neq 0$ and that with $\delta = 0$, divided by errors. We show that the optimal muon energy and baseline vary depending on the magnitude of θ_{13} , the background fraction and the uncertainty of the matter effect. In section 3 we discuss T violation assuming ideal polarization. In section 4 we present analytical treatments of the two kinds of $\Delta\chi^2$ introduced in sections 2 and 3, and show that these $\Delta\chi^2$ decrease as the muon energy becomes very small or very large. In section 5 we discuss the possibility of measurement of CP violation at the upgraded JHF experiment. In section 6 we summarize our results and we briefly comment on the uncertainty of the matter effects from the viewpoint of geophysics.

II. ANALYSIS OF CP VIOLATION

²Some of the correlations of errors of δ and other oscillation parameters have been discussed in the past [22,29], but they used relatively optimistic sets of the oscillation parameters, and the behaviors we obtain with the most up to date best fit values for the oscillation parameters are sometimes different from theirs.

A. Definition of $\Delta\chi^2$

Our strategy here is to examine whether a hypothesis with a vanishing CP phase is rejected or not by taking into consideration all channels $\nu_e \rightarrow \nu_\mu$, $\bar{\nu}_e \rightarrow \bar{\nu}_\mu$, $\nu_\mu \rightarrow \nu_\mu$ and $\bar{\nu}_\mu \rightarrow \bar{\nu}_\mu$. For this purpose we define $\Delta\chi^2$ to test a hypothesis that a CP phase is given by $\bar{\delta}$ in the case where the true value is δ :

$$\begin{aligned}
& \Delta\chi^2(\theta_{k\ell}, \Delta m_{k\ell}^2, \delta, C; \bar{\theta}_{k\ell}, \overline{\Delta m_{k\ell}^2}, \bar{\delta}, \bar{C}) \\
& \equiv \sum_j \frac{[N_j^{\text{wrong}}(\mu^-; \theta_{k\ell}, \Delta m_{k\ell}^2, \delta, C) - N_j^{\text{wrong}}(\mu^-; \bar{\theta}_{k\ell}, \overline{\Delta m_{k\ell}^2}, \bar{\delta}, \bar{C})]^2}{N_j^{\text{wrong}}(\mu^-; \theta_{k\ell}, \Delta m_{k\ell}^2, \delta, C)} \\
& + \sum_j \frac{[N_j^{\text{wrong}}(\mu^+; \theta_{k\ell}, \Delta m_{k\ell}^2, \delta, C) - N_j^{\text{wrong}}(\mu^+; \bar{\theta}_{k\ell}, \overline{\Delta m_{k\ell}^2}, \bar{\delta}, \bar{C})]^2}{N_j^{\text{wrong}}(\mu^+; \theta_{k\ell}, \Delta m_{k\ell}^2, \delta, C)} \\
& + \sum_j \frac{[N_j^{\text{right}}(\mu^-; \theta_{k\ell}, \Delta m_{k\ell}^2, \delta, C) - N_j^{\text{right}}(\mu^-; \bar{\theta}_{k\ell}, \overline{\Delta m_{k\ell}^2}, \bar{\delta}, \bar{C})]^2}{N_j^{\text{right}}(\mu^-; \theta_{k\ell}, \Delta m_{k\ell}^2, \delta, C)} \\
& + \sum_j \frac{[N_j^{\text{right}}(\mu^+; \theta_{k\ell}, \Delta m_{k\ell}^2, \delta, C) - N_j^{\text{right}}(\mu^+; \bar{\theta}_{k\ell}, \overline{\Delta m_{k\ell}^2}, \bar{\delta}, \bar{C})]^2}{N_j^{\text{right}}(\mu^+; \theta_{k\ell}, \Delta m_{k\ell}^2, \delta, C)}, \tag{1}
\end{aligned}$$

where j runs over energy bins and the numbers of events are given by

$$\begin{aligned}
& N_j^{\text{wrong}}(\mu^-; \theta_{k\ell}, \Delta m_{k\ell}^2, \delta, C) \\
& = \frac{12N_0 E_\mu}{\pi L^2 m_\mu^2} \int_{E_j}^{E_{j+1}} dE_\nu \left(\frac{E_\nu}{E_\mu} \right)^2 \left(1 - \frac{E_\nu}{E_\mu} \right) \sigma_{\nu N}(E_\nu) P(\nu_e \rightarrow \nu_\mu; \theta_{k\ell}, \Delta m_{k\ell}^2, \delta, C) \\
& N_j^{\text{wrong}}(\mu^+; \theta_{k\ell}, \Delta m_{k\ell}^2, \delta, C) \\
& = \frac{12N_0 E_\mu}{\pi L^2 m_\mu^2} \int_{E_j}^{E_{j+1}} dE_{\bar{\nu}} \left(\frac{E_{\bar{\nu}}}{E_\mu} \right)^2 \left(1 - \frac{E_{\bar{\nu}}}{E_\mu} \right) \sigma_{\bar{\nu} N}(E_{\bar{\nu}}) P(\bar{\nu}_e \rightarrow \bar{\nu}_\mu; \theta_{k\ell}, \Delta m_{k\ell}^2, \delta, C) \\
& N_j^{\text{right}}(\mu^-; \theta_{k\ell}, \Delta m_{k\ell}^2, \delta, C) \\
& = \frac{2N_0 E_\mu}{\pi L^2 m_\mu^2} \int_{E_j}^{E_{j+1}} dE_\nu \left(\frac{E_\nu}{E_\mu} \right)^2 \left(3 - 2 \frac{E_\nu}{E_\mu} \right) \sigma_{\nu N}(E_\nu) P(\nu_\mu \rightarrow \nu_\mu; \theta_{k\ell}, \Delta m_{k\ell}^2, \delta, C) \\
& N_j^{\text{right}}(\mu^+; \theta_{k\ell}, \Delta m_{k\ell}^2, \delta, C) \\
& = \frac{2N_0 E_\mu}{\pi L^2 m_\mu^2} \int_{E_j}^{E_{j+1}} dE_{\bar{\nu}} \left(\frac{E_{\bar{\nu}}}{E_\mu} \right)^2 \left(3 - 2 \frac{E_{\bar{\nu}}}{E_\mu} \right) \sigma_{\bar{\nu} N}(E_{\bar{\nu}}) P(\bar{\nu}_\mu \rightarrow \bar{\nu}_\mu; \theta_{k\ell}, \Delta m_{k\ell}^2, \delta, C),
\end{aligned}$$

where E_μ is the muon energy, L is the length of the neutrino path, N_0 is the number of the target nucleons times the number of useful decays of muons, $\sigma_{\nu N}(E_\nu)$ and $\sigma_{\bar{\nu} N}(E_{\bar{\nu}})$ are the (anti-)neutrino nucleon cross sections. We adopt the cross section which is the sum of those [37] of the quasi elastic scattering, one pion production, and inelastic scattering, where double counting of the latter two is suitably subtracted [38]. Throughout this paper the threshold energy is assumed to be 0.1GeV which is close to what has been assumed for

liquid argon detectors [29] and which may be realized in possible mega ton water Cherenkov detectors [39,40].

The number of the free parameters in the present case is six (δ , θ_{12} , θ_{13} , θ_{23} , Δm_{21}^2 , Δm_{21}^2), but the density $N_e(x) = Y_e(x)\rho(x)$ of electrons is not known exactly ($Y_e(x)$ is the ratio of the number of electrons to that of protons and neutrons, and $\rho(x)$ is the density of the Earth at a distance x from the beam production point), so we have to vary $N_e(x)$ also. Here for simplicity we assume the PREM (Preliminary Reference Earth Model) [41] and vary the overall normalization of the PREM:

$$A(x) = CA_0(x) = \sqrt{2}CG_F Y_e(x)N_e(x),$$

where $C = 1$ corresponds to the PREM. We have to consider correlations of errors of the CP phase and six other quantities and taking into account all these errors we obtain the probability of rejecting a hypothesis $\bar{\delta} = 0$. To do that we look for the minimum value of $\Delta\chi^2(\theta_{k\ell}, \Delta m_{k\ell}^2, \delta, C; \bar{\theta}_{k\ell}, \overline{\Delta m_{k\ell}^2}, \bar{\delta}, \bar{C})$ by varying the six parameters ($\bar{\theta}_{12}$, $\bar{\theta}_{13}$, $\bar{\theta}_{23}$, $\overline{\Delta m_{21}^2}$, $\overline{\Delta m_{32}^2}$, \bar{C}):

$$\Delta\chi_{\min}^2 \equiv \min_{\bar{\theta}_{k\ell}, \overline{\Delta m_{k\ell}^2}, \bar{C}} \Delta\chi^2(\theta_{k\ell}, \Delta m_{k\ell}^2, \delta, C; \bar{\theta}_{k\ell}, \overline{\Delta m_{k\ell}^2}, \bar{\delta} = 0, \bar{C}),$$

where C stands for the overall normalization of the electron density.

B. Correlations of errors of δ and other parameters

Let us first discuss correlations of two variables ($\bar{\delta}$, \bar{X}) where a parameter X stands for C , θ_{13} , θ_{12} , θ_{23} , Δm_{21}^2 and Δm_{32}^2 .

We have studied numerically correlations of errors between δ and the other oscillation parameters ($\theta_{k\ell}$, $\Delta m_{k\ell}^2$) as well as the normalization C of the matter effect for the case where the central values for these parameters are those of the best fit point, i.e., $\sin^2 2\theta_{12} = 0.75$, $\Delta m_{21}^2 = 3.2 \times 10^{-5} \text{eV}^2$; $\sin^2 2\theta_{23} = 1.0$, $\Delta m_{32}^2 = 3.2 \times 10^{-3} \text{eV}^2$, $C=1.0$ and we have used a reference value 8° . The values of $\Delta\chi^2(\theta_{12}, \theta_{13}, \theta_{23}, \Delta m_{21}^2, \Delta m_{32}^2, \delta, C; \theta_{12}, \theta_{13}, \theta_{23}, \Delta m_{21}^2, \Delta m_{32}^2, \bar{\delta}, \bar{C})$, $\Delta\chi^2(\theta_{12}, \theta_{13}, \theta_{23}, \Delta m_{21}^2, \Delta m_{32}^2, \delta, C; \theta_{12}, \bar{\theta}_{13}, \theta_{23}, \Delta m_{21}^2, \Delta m_{32}^2, \bar{\delta}, \bar{C})$, $\Delta\chi^2(\theta_{12}, \theta_{13}, \theta_{23}, \Delta m_{21}^2, \Delta m_{32}^2, \delta, C; \bar{\theta}_{12}, \theta_{13}, \theta_{23}, \Delta m_{21}^2, \Delta m_{32}^2, \bar{\delta}, \bar{C})$, $\Delta\chi^2(\theta_{12}, \theta_{13}, \theta_{23}, \Delta m_{21}^2, \Delta m_{32}^2, \delta, C; \theta_{12}, \theta_{13}, \bar{\theta}_{23}, \Delta m_{21}^2, \Delta m_{32}^2, \bar{\delta}, \bar{C})$, $\Delta\chi^2(\theta_{12}, \theta_{13}, \theta_{23}, \Delta m_{21}^2, \Delta m_{32}^2, \delta, C; \theta_{12}, \theta_{13}, \theta_{23}, \overline{\Delta m_{21}^2}, \overline{\Delta m_{32}^2}, \bar{\delta}, \bar{C})$, $\Delta\chi^2(\theta_{12}, \theta_{13}, \theta_{23}, \Delta m_{21}^2, \Delta m_{32}^2, \delta, C; \theta_{12}, \theta_{13}, \theta_{23}, \Delta m_{21}^2, \overline{\Delta m_{32}^2}, \bar{\delta}, \bar{C})$ are plotted in Fig. 1 – 6 in the case of $\delta = \pi/2$ for $E_\mu=3, 20, 50 \text{ GeV}$, $L=100\text{km}, 1000\text{km}, 2500\text{km}, 6300\text{km}$, where the data size $10^{21}\mu\cdot 10\text{kt}$ is used as a reference value and no backgrounds are assumed. Since the number of degrees of freedom is 2, $\Delta\chi^2=0.18, 0.34, 0.73$ correspond to 1σ , 90%, 99% confidence level to reject a hypothesis with $\bar{\delta} = 0$.

As can be seen in Fig. 1, the correlation ($\bar{\delta}$, \bar{C}) for $L \sim 3000\text{km}$ is strong for $\theta_{13} = 8^\circ$. The correlation ($\bar{\delta}$, \bar{C}) turns out to be small for larger values of Δm_{21}^2 or for smaller value of θ_{13} (i.e., $\theta_{13} \lesssim 3^\circ$; See Fig. 1b), as the gradient of the ellipse in the ($\bar{\delta}$, \bar{C}) plane becomes smaller for larger values of Δm_{21}^2 . This is why strong correlations were not found in [29] where the set of parameters ($\sin^2 2\theta_{12} = 1.0$, $\Delta m_{21}^2 = 1.0 \times 10^{-4} \text{eV}^2$; $\sin^2 2\theta_{23} = 1.0$,

$\Delta m_{32}^2 = 3.5(5, 7) \times 10^{-3} \text{eV}^2$) and $\sin^2 2\theta_{13} = 0.05$, $E_\mu = 30 \text{GeV}$ were used. If we assume that the uncertainty in the overall normalization C is at most 5%, then the correlation $(\bar{\delta}, \bar{C})$ is not so serious, but if we assume that the uncertainty is as large as 20 % then the set of the parameters ($E_\mu \sim 50 \text{GeV}$, $L \sim 3000 \text{km}$) is not a good option. We will discuss this issue later.

From Figs. 2 – 6, we see that the correlations of $(\bar{\delta}, \bar{\theta}_{k\ell})$ and $(\bar{\delta}, \overline{\Delta m_{k\ell}^2})$ are not large for $L \gtrsim 1000 \text{km}$, $E_\mu \gtrsim 20 \text{GeV}$. As we will show analytically later, the value of $\Delta\chi^2(\theta_{k\ell}, \Delta m_{k\ell}^2, \delta, C; \bar{\theta}_{k\ell}, \overline{\Delta m_{k\ell}^2}, \bar{\delta} = 0, \bar{C})$ increases for $E_\mu \gg 50 \text{GeV}$ and $L \ll 1000 \text{km}$ unless we minimize it with respect to $\theta_{k\ell}$ and $\Delta m_{k\ell}^2$, but because of strong correlations in $(\bar{\delta}, \bar{\theta}_{13})$, $(\bar{\delta}, \bar{\theta}_{23})$ and $(\bar{\delta}, \overline{\Delta m_{32}^2})$, the value of $\Delta\chi_{\min}^2$, which is minimized with respect to $\theta_{k\ell}$ and $\Delta m_{k\ell}^2$, decreases for $E_\mu \gg 50 \text{GeV}$.

C. Data size to reject a hypothesis with $\bar{\delta} = 0$

The quantity $\Delta\chi_{\min}^2$ can be regarded as the deviation of χ^2 from the best fit point (the best fit point in eq. (1) is of course $\bar{\theta}_{k\ell} = \theta_{k\ell}$, $\overline{\Delta m_{k\ell}^2} = \Delta m_{k\ell}^2$, $\bar{\delta} = \delta$ and $\bar{C} = C$ for which we have $\Delta\chi_{\min}^2 = 0$) and for six degrees of freedom the value of $\Delta\chi_{\min}^2$ which corresponds to 3σ (4σ) is 20.1 (28.9). From this we can estimate the necessary data size D to reject a hypothesis $\bar{\delta} = 0$ at 3σ by dividing 20.1 by $\Delta\chi_{\min}^2$ for each value of δ . On the other hand, it is important to include the effect of the backgrounds in the analysis [22,29,42]. Here we assume that the fraction f_B of backgrounds to right sign muon events is given by $f_B = 10^{-3}$ or 10^{-5} and that the systematic error of backgrounds is $\sigma_B = 0.1$ as in [42] for simplicity. We also assume the number of muons $10^{21} \mu \cdot 10 \text{kt}$ as a reference value. Thus $\Delta\chi^2$ is modified as

$$\begin{aligned} & \Delta\chi^2(\theta_{k\ell}, \Delta m_{k\ell}^2, \delta, C; \bar{\theta}_{k\ell}, \overline{\Delta m_{k\ell}^2}, \bar{\delta}, \bar{C}) \Big|_{f_B} \\ & \equiv \sum_j \frac{[N_j^{\text{wrong}}(\mu^-) - \bar{N}_j^{\text{wrong}}(\mu^-)]^2}{\left[\sqrt{N_j^{\text{wrong}}(\mu^-) + f_B N_j^{\text{right}}(\mu^+) + 1 + \frac{11}{9}} \right]^2 + [\sigma_B f_B N_j^{\text{right}}(\mu^+)]^2} \\ & + \sum_j \frac{[N_j^{\text{wrong}}(\mu^+) - \bar{N}_j^{\text{wrong}}(\mu^+)]^2}{\left[\sqrt{N_j^{\text{wrong}}(\mu^+) + f_B N_j^{\text{right}}(\mu^-) + 1 + \frac{11}{9}} \right]^2 + [\sigma_B f_B N_j^{\text{right}}(\mu^-)]^2} \\ & + \sum_j \frac{[N_j^{\text{right}}(\mu^-) - \bar{N}_j^{\text{right}}(\mu^-)]^2}{N_j^{\text{right}}(\mu^-)} + \sum_j \frac{[N_j^{\text{right}}(\mu^+) - \bar{N}_j^{\text{right}}(\mu^+)]^2}{N_j^{\text{right}}(\mu^+)}, \end{aligned} \quad (2)$$

where $\bar{N}_j^{\text{wrong}}(\mu^\pm)$, $\bar{N}_j^{\text{right}}(\mu^\pm)$ stand for $N_j^{\text{wrong}}(\mu^\pm)$, $N_j^{\text{right}}(\mu^\pm)$ with arguments $\bar{\theta}_{k\ell}, \overline{\Delta m_{k\ell}^2}, \bar{\delta}, \bar{C}$, respectively, and the corrections in the statistical errors are due to the Poisson statistical [42]. Then we minimize $\Delta\chi^2$ with respect $\bar{\theta}_{k\ell}$, $\overline{\Delta m_{k\ell}^2}$ and \bar{C} :

$$\Delta\chi_{\min}^2 \Big|_{f_B} \equiv \min_{\bar{\theta}_{k\ell}, \overline{\Delta m_{k\ell}^2}, \bar{C}} \Delta\chi^2(\theta_{k\ell}, \Delta m_{k\ell}^2, \delta, C; \bar{\theta}_{k\ell}, \overline{\Delta m_{k\ell}^2}, \bar{\delta} = 0, \bar{C}) \Big|_{f_B}, \quad (3)$$

where the values of oscillation parameters we use in (3) are the best fit values in the analyses of the solar and atmospheric neutrinos [43] as in Figs. 1 – 6, and we take $\theta_{13}=1^\circ, 5^\circ, 8^\circ$ and $\delta = \pi/2$ as a reference value. In varying the overall normalization C we assume $0.95 \leq C \leq 1.05$. We will mention the results for $|\Delta C| \leq 0.1$ and for $|\Delta C| \leq 0.2$ later. For other oscillation parameters, we vary $(\theta_{12}, \Delta m_{21}^2)$ and $(\theta_{23}, \Delta m_{32}^2)$ within the allowed region at 90%CL of the solar and the atmospheric neutrino data, i.e., $25^\circ \leq \theta_{12} \leq 41^\circ$, $35^\circ \leq \theta_{23} \leq 55^\circ$, $1.5 \times 10^{-5} \text{eV}^2 \leq \Delta m_{21}^2 \leq 2.2 \times 10^{-4} \text{eV}^2$, $1.6 \times 10^{-3} \text{eV}^2 \leq \Delta m_{32}^2 \leq 4 \times 10^{-3} \text{eV}^2$. It should be emphasized that in minimizing $\Delta\chi^2$ in (3) all the six parameters are varied at the same time, unlike in Figs. 1 – 6 which are obtained by varying only one of $\bar{\theta}_{\ell\ell}$, $\overline{\Delta m_{\ell\ell}^2}$, \bar{C} .

The result is given in Fig. 7 for a neutrino factory with $0.5 \text{GeV} \leq E_\mu \leq 50 \text{GeV}$, $10 \text{km} \leq L \leq 10000 \text{km}$ and for three values of $\theta_{13}=1^\circ, 5^\circ, 8^\circ$ and two different values of the background fraction $f_B = 10^{-5}, 10^{-3}$. The behavior of the figures change a little depending on the value of θ_{13} . For $f_B = 10^{-3}$, the sensitivity to CP violation, i.e., the ability to reject a hypothesis with $\bar{\delta} = 0$ is *not* optimized by the set of parameters $(E_\mu, L) \simeq (50 \text{GeV}, 3000 \text{km})$, which has been advocated as the best choice, but rather by $(E_\mu, L) \simeq (20 \text{GeV}, 2000 \text{km})$. This is because with a nonnegligible fraction f_B the contribution of the systematic uncertainty $\sigma_B f_B N_j^{\text{right}}$ to the total error becomes so large for high energy such as $E_\mu \sim 50 \text{GeV}$ and sensitivity to CP violation is lost. For $f_B = 10^{-5}$ and $\theta_{13}=1^\circ$, on the other hand, the contribution of $\sigma_B f_B N_j^{\text{right}}$ is not so large and the sensitivity is optimized by $(E_\mu, L) \simeq (50 \text{GeV}, 3000 \text{km})$. We note in passing that we have also optimized the sensitivity with respect to the number of energy bins but the conclusion does not depend very much on the number of energy bins. This result disagrees with the claim in [32].

We have also evaluated the data size assuming a larger uncertainty of the matter effect, i.e., $|\Delta C| \leq 0.1$ and $|\Delta C| \leq 0.2$. The results for $\theta_{13} = 8^\circ$ are shown in Fig. 8. If we have to assume an uncertainty of the matter effect which is as large as 20%, then the optimum baseline and muon energy become even smaller than the results with $|\Delta C| \leq 0.05$. The situation is less serious for smaller value of θ_{13} , i.e., $\theta_{13} \lesssim 3^\circ$, for which the correlation $(\bar{\delta}, \bar{C})$ is not so strong. It should be noted that we have assumed in our analysis that the detection efficiency does not decrease down to the neutrino energy $E_\nu \sim$ a few GeV, so if this assumption is not satisfied then the optimum muon energy may not be as low as Fig. 8 indicates.

In Figs. 7 and 8 we have taken $\delta = \pi/2$ as a reference value. It is possible to do the same analysis for a value of δ other than $\pi/2$. The results for $\theta_{13}=8^\circ, 5^\circ$ and 1° are given in Fig. 9 for three sets of the parameters $(E_\mu=50 \text{GeV}, L=3000 \text{km})$, $(E_\mu=20 \text{GeV}, L=1000 \text{km})$ and $(E_\mu=20 \text{GeV}, L=2000 \text{km})$. We observe that $(E_\mu=50 \text{GeV}, L=3000 \text{km})$ is better than $(E_\mu=20 \text{GeV}, L=1000 \text{km})$ for smaller values of θ_{13} , but for larger values of θ_{13} $(E_\mu=20 \text{GeV}, L=1000 \text{km})$ can be more advantageous than the other. It should be emphasized that in all cases in Fig. 9 we can distinguish the case of $\delta = \pi$ from that of $\delta = 0$, since the necessary data size to reject $\delta = 0$ is finite even for $\delta = \pi$. This is because there are both contributions from $\sin \delta$ and $\cos \delta$ for the muon energy $E_\mu \lesssim 50 \text{GeV}$. As we will see in section 4, for extremely high energy $E_\mu \gg 50 \text{GeV}$ we can show analytically that our $\Delta\chi^2(\text{CPV})$ becomes proportional to $\sin^2 \delta$ and distinction between $\delta = \pi$ and $\delta = 0$ is no longer possible.

Sato et al. [32] have been emphasizing the importance of the low energy option ($E_\mu \lesssim 1 \text{GeV}$), since the shape of sine curves in the CP violating probabilities becomes more conspicuous for low energies. As can be seen from Fig. 7, the data set which is require to

reject a hypothesis $\bar{\delta} = 0$ is much larger than the value for the high energy case. This is because the small boost factor $(E_\mu/m_\mu)^2$ means that the number of events is statistically insufficient even though the CP conserving probabilities become relatively large in this case. Furthermore, in obtaining Fig. 7, we have assumed that the detection efficiency does not change for low energy. In reality, however, it becomes more and more difficult to distinguish wrong sign muons from right sign ones at lower energy so that the background fraction is expected to increase as $E_\mu \rightarrow$ small. Therefore, we conclude that the low energy option offers no advantage over the high energy region as long as we have the same detector size.

Sato et al. [32] gave another criticism that neutrino factories at high energy are looking at only terms which are proportional to $\cos\delta$. However, as we will see in section 4, we can show analytically in the high energy limit that our $\Delta\chi^2(\text{CPV})$, when minimized with respect to one of the oscillation parameters, is proportional to the square J^2 of the Jarlskog factor and has the same behavior $\propto 1/E_\mu$ as $\Delta\chi^2$ in the case of T violation. Therefore a naive argument that the square of difference of the quantity at δ and the one at $\delta = 0$ must depend only on $\cos\delta$ does not necessarily apply.

III. ANALYSIS OF T VIOLATION

It is known that measurements of T violation at neutrino factories are very difficult since electrons and positrons are difficult to distinguish at high energy. Here we discuss the possibility of measurements of T violation assuming perfect polarized muon beams for simplicity, i.e., $P_\mu \cos\theta$ in eqs. (3) and (4) in [19] is assumed to be ± 1 so that either the flux of ν_e or $\bar{\nu}_e$ vanishes. If we assume $P_\mu \cos\theta = -1$, then we have

$$\begin{aligned} \left. \frac{d^2 N_{\bar{\nu}_e}}{dx d\Omega} \right|_{P_\mu \cos\theta = -1} &= 0 \\ \left. \frac{d^2 N_{\nu_\mu}}{dx d\Omega} \right|_{P_\mu \cos\theta = -1} &= \frac{2x^2}{4\pi} [(3 - 2x) + (1 - 2x)] = \frac{2}{3} \left. \frac{d^2 N_{\bar{\nu}_e}}{dx d\Omega} \right|_{P_\mu \cos\theta = 0}, \end{aligned} \quad (4)$$

where $x \equiv E_\nu/E_\mu$, so that we can compare the numbers of events $(3/2)N_j(\nu_\mu \rightarrow \nu_e; P_\mu \cos\theta = -1)$ from ν_μ in decays of polarized μ^- and $N_j(\nu_e \rightarrow \nu_\mu; P_\mu \cos\theta = 0)$ from ν_e in decays of unpolarized μ^+ . $\Delta\chi^2$ in this case is thus given by

$$\Delta\chi^2(\text{TV})|_{f_B} \equiv \sum_j \frac{[N_j(\nu_e \rightarrow \nu_\mu; P_\mu \cos\theta = 0) - \frac{3}{2}N_j(\nu_\mu \rightarrow \nu_e; P_\mu \cos\theta = -1)]^2}{\Delta N^2}, \quad (5)$$

where

$$\begin{aligned} N_j(\nu_\mu \rightarrow \nu_e; P_\mu \cos\theta = -1) &\equiv \frac{8N_0 E_\mu}{\pi L^2 m_\mu^2} \int_{E_j}^{E_{j+1}} dE_\nu \left(\frac{E_\nu}{E_\mu} \right)^2 \left(1 - \frac{E_\nu}{E_\mu} \right) \sigma_{\nu N}(E_\nu) P(\nu_\mu \rightarrow \nu_e) \\ N_j(\nu_e \rightarrow \nu_\mu; P_\mu \cos\theta = 0) &\equiv \frac{12N_0 E_\mu}{\pi L^2 m_\mu^2} \int_{E_j}^{E_{j+1}} dE_\nu \left(\frac{E_\nu}{E_\mu} \right)^2 \left(1 - \frac{E_\nu}{E_\mu} \right) \sigma_{\nu N}(E_\nu) P(\nu_e \rightarrow \nu_\mu) \\ \Delta N^2 &\equiv \left[\sqrt{N_j(\nu_e \rightarrow \nu_\mu; P_\mu \cos\theta = 0) + f_B N_j(\bar{\nu}_\mu \rightarrow \bar{\nu}_\mu; P_\mu \cos\theta = 0) + 1} + \frac{11}{9} \right]^2 \\ &\quad + \left(\frac{3}{2} \right)^2 N_j(\nu_\mu \rightarrow \nu_e; P_\mu \cos\theta = -1) + [\sigma_B f_B N_j(\bar{\nu}_\mu \rightarrow \bar{\nu}_\mu; P_\mu \cos\theta = 0)]^2 \end{aligned} \quad (6)$$

and the systematic errors are taken into account only for the μ^+ beam. In the definition (5) we do not optimize $\Delta\chi^2(\text{TV})$ with respect to $\theta_{k\ell}$, $\Delta m_{k\ell}^2$, C , since the numerator is defined only by quantities which are measured by experiments and a non zero value of $\Delta\chi^2(\text{TV})$ immediately indicates $\delta \neq 0$. The data size to reject a hypothesis with $\bar{\delta} = 0$ at 3σ using $\Delta\chi^2(\text{TV})$ can be calculated as in the case of $\Delta\chi^2(\text{CPV})$ and is shown in Fig. 10 for $\delta = \pi/2$ and $\theta_{13} = 8^\circ$ assuming the best fit values for $(\theta_{12}, \Delta m_{21}^2)$ and $(\theta_{23}, \Delta m_{32}^2)$. The number of degrees of freedom in this case is one, i.e., the magnitude of the Jarlskog factor $J \equiv \tilde{J} \sin \delta$, so that the data size is in general smaller than the case of CP violation for which we have six degrees of freedom. In practice, however, obtaining $P_\mu \cos \theta \simeq \pm 1$ is technically difficult and the possibility to use T violation seems to be challenging.

IV. LOW AND HIGH ENERGY BEHAVIORS OF $\Delta\chi^2$

In this subsection we will show analytically that the sensitivity to CP and T violation decreases as $E_\mu \rightarrow \text{small}$ ($E_\mu \ll 10\text{GeV}$) or $E_\mu \rightarrow \text{large}$ ($E_\mu \gg 50\text{GeV}$). Throughout this paper we assume $\sin^2 2\theta_{13} \gtrsim 10^{-3}$ ($\theta_{13} \gtrsim 1^\circ$) so that we are always in the atmospheric regime in the language of [44], i.e., $\sin^2 2\theta_{13} / \sin^2 2\theta_{12} \gg (\Delta m_{21}^2 / \Delta m_{31}^2)^2$. In this subsection we will ignore the effects of backgrounds and systematic errors for simplicity.

To examine significance of CP/T violation analytically, we introduce the following simplified quantities:

$$\begin{aligned} \Delta\chi^2(\text{CPV}) &\equiv \min_{\bar{\theta}_{k\ell}, \bar{\Delta m_{k\ell}^2}, \bar{C}} \Delta\chi^2(\theta_{k\ell}, \Delta m_{k\ell}^2, \delta, C; \bar{\theta}_{k\ell}, \bar{\Delta m_{k\ell}^2}, \bar{\delta} = 0, \bar{C}), \\ \Delta\chi^2(\text{TV}) &\equiv \frac{[\langle P(\nu_e \rightarrow \nu_\mu; \delta) \rangle - \langle P(\nu_\mu \rightarrow \nu_e; \delta) \rangle]^2}{\langle P(\nu_e \rightarrow \nu_\mu; \delta) \rangle}, \end{aligned} \quad (7)$$

where

$$\begin{aligned} &\Delta\chi^2(\theta_{k\ell}, \Delta m_{k\ell}^2, \delta, C; \bar{\theta}_{k\ell}, \bar{\Delta m_{k\ell}^2}, \bar{\delta}, \bar{C}) \\ &= \frac{[\langle P(\nu_e \rightarrow \nu_\mu; \theta_{k\ell}, \Delta m_{k\ell}^2, \delta, C) \rangle - \langle P(\nu_e \rightarrow \nu_\mu; \bar{\theta}_{k\ell}, \bar{\Delta m_{k\ell}^2}, \bar{\delta}, \bar{C}) \rangle]^2}{\langle P(\nu_e \rightarrow \nu_\mu; \delta) \rangle} \end{aligned} \quad (8)$$

is defined as in (1),

$$\langle P(\nu_\alpha \rightarrow \nu_\beta; \delta) \rangle \equiv \frac{12N_0 E_\mu^2}{\pi L^2 m_\mu^2} \int d\left(\frac{E_\nu}{E_\mu}\right) \left(\frac{E_\nu}{E_\mu}\right)^2 \left(1 - \frac{E_\nu}{E_\mu}\right) \sigma_{\nu N}(E_\nu) P(\nu_\alpha \rightarrow \nu_\beta; \delta) \quad (9)$$

are the number of events $((\alpha, \beta) = (e, \mu) \text{ or } (\mu, e))$; in the case of $(\alpha, \beta) = (\mu, e)$ we assume perfect polarization as in the previous section so that the number of events is given by the same definition (9) and we have ignored effects of the backgrounds and systematic errors and correlations of errors for simplicity in this section. Also we will assume that the cross section is proportional to the neutrino energy E_ν for any E_ν , i.e., $\sigma = \sigma_0 E_\nu$. Strictly speaking this assumption is not accurate, but it is known [38] that $0 < \sigma < \sigma_0 E_\nu$ is satisfied for low energy $E_\nu \ll 1\text{GeV}$, so our approximation is sufficient to give an upper bound on the value of $\Delta\chi^2$ for low energy.

Let us first look at the low energy limit ($E_\nu \ll 10\text{GeV}$). In this case matter effects are negligible and the probability can be replaced by that in vacuum. Thus we have

$$P(\nu_e \rightarrow \nu_\mu; \delta) \simeq s_{23}^2 \sin^2 2\theta_{13} \sin\left(\frac{\Delta E_{31}L}{2}\right) + c_{23}^2 \sin^2 2\theta_{12} \sin\left(\frac{\Delta E_{21}L}{2}\right) + 8\tilde{J} \sin\left(\frac{\Delta E_{21}L}{2}\right) \sin\left(\frac{\Delta E_{31}L}{2}\right) \cos\left(\delta + \frac{\Delta E_{31}L}{2}\right) \quad (10)$$

to the second order in $\mathcal{O}(\theta_{13})$ and $\mathcal{O}(\Delta E_{21}/\Delta E_{31})$, where

$$\tilde{J} \equiv \frac{c_{13}}{8} \sin 2\theta_{12} \sin 2\theta_{13} \sin 2\theta_{23}, \quad (11)$$

and $\Delta E_{jk} \equiv \Delta m_{jk}^2/2E \equiv (m_j^2 - m_k^2)/2E$. The number of events are given by

$$\begin{aligned} & \langle P(\nu_e \rightarrow \nu_\mu; \delta) \rangle - \langle P(\nu_e \rightarrow \nu_\mu; \delta = 0) \rangle \\ &= \frac{96N_0 E_\mu^3 \sigma_0 \tilde{J}}{\pi L^2 m_\mu^2} \int dx x^3 (1-x) \sin\left(\frac{\Delta m_{21}^2 L}{4x E_\mu}\right) \\ & \times \sin\left(\frac{\Delta m_{31}^2 L}{4x E_\mu}\right) \left[\cos\left(\delta + \frac{\Delta m_{31}^2 L}{4x E_\mu}\right) - \cos\left(\frac{\Delta m_{31}^2 L}{4x E_\mu}\right) \right] \end{aligned} \quad (12)$$

$$\begin{aligned} & \langle P(\nu_e \rightarrow \nu_\mu; \delta) \rangle - \langle P(\nu_\mu \rightarrow \nu_e; \delta) \rangle \\ &= \frac{192N_0 E_\mu^3 \sigma_0 \tilde{J} \sin \delta}{\pi L^2 m_\mu^2} \int dx x^3 (1-x) \sin\left(\frac{\Delta m_{21}^2 L}{4x E_\mu}\right) \sin\left(\frac{\Delta m_{31}^2 L}{4x E_\mu}\right) \sin\left(\frac{\Delta m_{32}^2 L}{4x E_\mu}\right) \end{aligned} \quad (13)$$

$$\begin{aligned} & \langle P(\nu_e \rightarrow \nu_\mu; \delta) \rangle \\ & \simeq \frac{12s_{23}^2 \sin^2 2\theta_{13} E_\mu^3 \sigma_0}{\pi L^2 m_\mu^2} \int dx x^3 (1-x) \sin^2\left(\frac{\Delta m_{31}^2 L}{4x E_\mu}\right), \end{aligned} \quad (14)$$

where $x \equiv E_\nu/E_\mu$, we have assumed conditions for the atmospheric regime $\sin^2 2\theta_{13}/\sin^2 2\theta_{12} \gg (\Delta m_{21}^2/\Delta m_{21}^2)^2$, and we have put $\bar{\theta}_{k\ell} = \theta_{k\ell}$, $\overline{\Delta m_{k\ell}^2} = \Delta m_{k\ell}^2$, $\bar{C} = C$ in (12) instead of optimizing $\langle P(\nu_e \rightarrow \nu_\mu; \delta) \rangle - \langle P(\nu_e \rightarrow \nu_\mu; \delta = 0) \rangle$ with respect to these variables, as that is sufficient to demonstrate that $\Delta\chi^2(\text{CPV})$ decreases as $E_\mu \rightarrow 0$. If we keep L/E_μ fixed while $L, E_\mu \rightarrow \text{small}$, then all the quantities (12), (13) and (14) behave as $\mathcal{O}(E_\mu)$, so $\Delta\chi^2(\text{CPV}) \propto E_\mu$ and $\Delta\chi^2(\text{TV}) \propto E_\mu$ as $E_\mu \rightarrow 0$ with L/E_μ fixed. Thus sensitivity to CP/T violation is asymptotically lost as $E_\mu \rightarrow 0$. This is consistent with our numerical results in previous sections.

Next let us discuss the behavior of $\Delta\chi^2$ in the high energy limit ($E_\mu \gg 50\text{GeV}$). In this case we have to take into account the matter effect and we use the probability which has been obtained in [22] to second order in $\mathcal{O}(\theta_{13})$, $\mathcal{O}(\Delta E_{21}/\Delta E_{31})$, $\mathcal{O}(\Delta E_{21}/A)$ and $\mathcal{O}(\Delta E_{21}L)$:

$$\begin{aligned} P(\nu_e \rightarrow \nu_\mu; \delta) & \simeq s_{23}^2 \sin^2 2\theta_{13} \left(\frac{\Delta E_{31}}{B}\right)^2 \sin^2\left(\frac{BL}{2}\right) + c_{23}^2 \sin^2 2\theta_{12} \left(\frac{\Delta E_{21}}{A}\right)^2 \sin^2\left(\frac{AL}{2}\right) \\ & + 8\tilde{J} \frac{\Delta E_{21}}{A} \frac{\Delta E_{31}}{B} \sin\left(\frac{AL}{2}\right) \sin\left(\frac{BL}{2}\right) \cos\left(\delta + \frac{\Delta E_{31}L}{2}\right). \end{aligned} \quad (15)$$

Since we assume $\sin^2 2\theta_{13}/\sin^2 2\theta_{12} \gg (\Delta m_{21}^2/\Delta m_{21}^2)^2 = (\Delta E_{21}/\Delta E_{31})^2$ here, we can ignore the second term in (15).

It is straightforward to get the following high energy limit of $\Delta\chi^2(\text{TV})$. Using (15) we have

$$\begin{aligned} P(\nu_e \rightarrow \nu_\mu; \delta) - P(\nu_\mu \rightarrow \nu_e; \delta) &= P(\nu_e \rightarrow \nu_\mu; \delta) - P(\nu_e \rightarrow \nu_\mu; -\delta) \\ &\simeq -2\tilde{J} \frac{\Delta m_{21}^2 (\Delta m_{31}^2)^2}{E_\nu^3} \frac{L}{A^2} \sin^2 \left(\frac{AL}{2} \right), \end{aligned} \quad (16)$$

where we have expanded $\sin(\Delta E_{21}L/2) \simeq \Delta E_{21}L/2$ and have used the fact $B = [(\Delta E_{31} \cos 2\theta_{13} - A)^2 + (\Delta E_{31} \sin 2\theta_{13})^2]^{1/2} \simeq A$ as $E_\nu \rightarrow \text{large}$. Therefore the number of events is given by

$$\begin{aligned} &\langle P(\nu_e \rightarrow \nu_\mu; \delta) \rangle - \langle P(\nu_\mu \rightarrow \nu_e; \delta) \rangle \\ &\simeq \frac{24N_0\sigma_0\tilde{J} \sin \delta \Delta m_{21}^2 (\Delta m_{31}^2)^2}{\pi m_\mu^2} \frac{1}{A^2 L} \sin^2 \left(\frac{AL}{2} \right) \int dx (1-x) \\ &= \frac{12N_0\sigma_0\tilde{J} \sin \delta \Delta m_{21}^2 (\Delta m_{31}^2)^2}{\pi m_\mu^2} \frac{1}{A^2 L} \sin^2 \left(\frac{AL}{2} \right), \end{aligned} \quad (17)$$

$$\begin{aligned} &\langle P(\nu_e \rightarrow \nu_\mu; \delta) \rangle \\ &\simeq \frac{3N_0\sigma_0 s_{23}^2 \sin^2 2\theta_{13}}{\pi m_\mu^2} \frac{E_\mu}{A^2 L^2} \sin^2 \left(\frac{AL}{2} \right) \int dx x(1-x) \\ &= \frac{N_0\sigma_0 s_{23}^2 \sin^2 2\theta_{13}}{2\pi m_\mu^2} \frac{E_\mu}{A^2 L^2} \sin^2 \left(\frac{AL}{2} \right). \end{aligned} \quad (18)$$

Hence we have the behaviors

$$\begin{aligned} \Delta\chi^2(\text{TV}) &\simeq \frac{N_0\sigma_0}{\pi m_\mu^2} \frac{288 \sin^2 \delta \tilde{J}^2 (\Delta m_{21}^2)^2 (\Delta m_{31}^2)^4}{s_{23}^2 \sin^2 2\theta_{13}} \frac{1}{E_\mu A^2} \sin^2 \left(\frac{AL}{2} \right) \\ &\text{as } E_\mu \rightarrow \text{large}. \end{aligned} \quad (19)$$

(19) indicates that the sensitivity to T violation decreases as E_μ becomes very large. Also for a fixed large E_μ , $\Delta\chi^2(\text{TV})$ is optimized for $L \sim \pi/A \sim 3 \times 2000 \text{km}/(\rho/2.7 \text{g}\cdot\text{cm}^{-3}) \sim 5000 \text{km}$. From numerical calculations we see that $\Delta\chi^2(\text{TV})$ is optimized for $(L, E_\mu) \sim (3000 \text{km}, 50 \text{GeV})$ (see Fig. 1), so our analytic treatment is consistent with numerical calculations qualitatively.

The behavior of $\Delta\chi^2(\text{CPV})$ is a little more complicated, as we have to optimize $\Delta\chi^2$ with respect to $\bar{\theta}_{k\ell}$, $\bar{\Delta m_{k\ell}^2}$, \bar{C} . If we put $\bar{\theta}_{k\ell} = \theta_{k\ell}$, $\bar{\Delta m_{k\ell}^2} = \Delta m_{k\ell}^2$, $\bar{C} = C$ as we did in (12), we have

$$P(\nu_e \rightarrow \nu_\mu; \delta) - P(\nu_e \rightarrow \nu_\mu; \delta = 0) \simeq 2\tilde{J}(\cos \delta - 1) \frac{\Delta m_{21}^2 \Delta m_{31}^2}{E_\nu^2} \frac{1}{A^2} \sin^2 \left(\frac{AL}{2} \right), \quad (20)$$

$$\langle P(\nu_e \rightarrow \nu_\mu; \delta) \rangle - \langle P(\nu_e \rightarrow \nu_\mu; \delta = 0) \rangle = \frac{4N_0\sigma_0\tilde{J}(\cos \delta - 1)\Delta m_{21}^2 \Delta m_{31}^2}{\pi m_\mu^2} \frac{E_\mu}{A^2 L^2} \sin^2 \left(\frac{AL}{2} \right), \quad (21)$$

so that we naively have the following behavior

$$\Delta\chi^2(\text{naive CPV}) \simeq \frac{N_0\sigma_0}{\pi m_\mu^2} \frac{32(\cos\delta - 1)^2 \tilde{J}^2 (\Delta m_{21}^2)^2 (\Delta m_{31}^2)^2}{s_{23}^2 \sin^2 2\theta_{13}} \frac{E_\mu}{A^2 L^2} \sin^2\left(\frac{AL}{2}\right). \quad (22)$$

It turns out that it is sufficient to consider the correlation of two variables $(\bar{\delta}, \bar{X})$, where X is $\theta_{k\ell}$, $\Delta m_{k\ell}^2$ or C , to demonstrate $\Delta\chi^2(\text{CPV}) \propto 1/E_\mu$. Except for the correlations $(\bar{\delta}, \bar{\theta}_{12})$ and $(\bar{\delta}, \bar{\Delta m_{21}^2})$, we can ignore terms of order $\mathcal{O}((\Delta E_{21}/\Delta E_{31})^2)$. From the assumption $\sin^2 2\theta_{13}/\sin^2 2\theta_{12} \gg (\Delta m_{21}^2/\Delta m_{31}^2)^2$, (15) is approximately given by

$$P(\nu_e \rightarrow \nu_\mu; \delta) \simeq \left[s_{23} \sin 2\theta_{13} \frac{\Delta E_{31}}{A} \sin\left(\frac{AL}{2}\right) + \frac{4\tilde{J}}{s_{23} \sin 2\theta_{13}} \frac{\Delta E_{21}}{A} \sin\left(\frac{AL}{2}\right) \cos\left(\delta + \frac{\Delta E_{31}L}{2}\right) \right]^2, \quad (23)$$

where we have used $A - \Delta E_{31} \simeq A$ for $E_\nu \rightarrow \text{large}$, and we have ignored terms of order $\mathcal{O}((\Delta E_{21}/\Delta E_{31})^2)$. In the case of the two variable correlation $(\bar{\delta}, \bar{\theta}_{13})$, to minimize the square of

$$\begin{aligned} & P(\nu_e \rightarrow \nu_\mu; \theta_{13}, \delta) - P(\nu_e \rightarrow \nu_\mu; \bar{\theta}_{13}, \bar{\delta}) \\ & \simeq \left[s_{23} \sin 2\theta_{13} \frac{\Delta E_{31}}{A} \sin\left(\frac{AL}{2}\right) + \frac{4\tilde{J}}{s_{23} \sin 2\theta_{13}} \frac{\Delta E_{21}}{A} \sin\left(\frac{AL}{2}\right) \cos\left(\delta + \frac{\Delta E_{31}L}{2}\right) \right]^2 \\ & - \left[s_{23} \sin 2\bar{\theta}_{13} \frac{\Delta E_{31}}{A} \sin\left(\frac{AL}{2}\right) + \frac{4\tilde{J}}{s_{23} \sin 2\bar{\theta}_{13}} \frac{\Delta E_{21}}{A} \sin\left(\frac{AL}{2}\right) \cos\left(\bar{\delta} + \frac{\Delta E_{31}L}{2}\right) \right]^2, \end{aligned} \quad (24)$$

it is sufficient to take³

$$\sin 2\bar{\theta}_{13} = \sin 2\theta_{13} - \frac{4\tilde{J}}{s_{23}^2 \sin 2\theta_{13}} \frac{\Delta m_{21}^2}{\Delta m_{31}^2} (\cos \bar{\delta} - \cos \delta), \quad (25)$$

where we have used in (24) and (25) the fact $\tilde{J}/\sin 2\theta_{13} = \cos \theta_{13} \times (\text{independent of } \theta_{13}) \simeq \cos \bar{\theta}_{13} \times (\text{independent of } \theta_{13})$ which holds because $\sin^2 \theta_{13} \ll 1$. Notice that the phase $\Delta E_{31}L/2$ which appears together with δ in cosine in (24) disappears as $E_\nu \rightarrow \text{large}$. Plugging (25) in (24), we find

$$\begin{aligned} & P(\nu_e \rightarrow \nu_\mu; \theta_{13}, \delta) - P(\nu_e \rightarrow \nu_\mu; \bar{\theta}_{13}, \bar{\delta}) \\ & \simeq s_{23}^2 \left(\frac{\Delta E_{31}}{A} \right)^2 \sin^2\left(\frac{AL}{2}\right) (\sin^2 2\theta_{13} - \sin^2 2\bar{\theta}_{13}) \\ & + 8\tilde{J} \frac{\Delta E_{21} \Delta E_{31}}{A^2} \sin^2\left(\frac{AL}{2}\right) \left[\cos\left(\delta + \frac{\Delta E_{31}L}{2}\right) - \cos\left(\bar{\delta} + \frac{\Delta E_{31}L}{2}\right) \right], \\ & \simeq 8\tilde{J} \frac{\Delta E_{21} \Delta E_{31}}{A^2} \sin^2\left(\frac{AL}{2}\right) \\ & \times \left[\cos\left(\delta + \frac{\Delta E_{31}L}{2}\right) - \cos\left(\bar{\delta} + \frac{\Delta E_{31}L}{2}\right) - \cos \delta + \cos \bar{\delta} \right], \\ & \simeq 8\tilde{J} \frac{\Delta E_{21} \Delta E_{31}}{A^2} \sin^2\left(\frac{AL}{2}\right) (\sin \bar{\delta} - \sin \delta) \frac{\Delta E_{31}L}{2}, \end{aligned} \quad (26)$$

³ Here we do not discuss the other solution of the quadratic equation which was discussed by [44], since we are mainly interested in rejecting $\delta = 0$ rather than determining the precise value of δ .

where we have expanded $\sin(\Delta E_{31}L/2) \simeq \Delta E_{31}L/2$, $\cos(\Delta E_{31}L/2) - 1 \simeq -(\Delta E_{31}L)^2/2 \simeq 0$ in the last step in (26). Hence we get

$$\begin{aligned} & \left\langle P(\nu_e \rightarrow \nu_\mu; \theta_{13}, \delta) - P(\nu_e \rightarrow \nu_\mu; \bar{\theta}_{13}, \bar{\delta} = 0) \right\rangle \\ & \simeq -\frac{6N_0\sigma_0}{\pi m_\mu^2} \tilde{J} \sin \delta \frac{\Delta m_{21}^2 (\Delta m_{31}^2)^2}{A^2 L^2} \sin^2 \left(\frac{AL}{2} \right) \int dx (1-x) \\ & = \frac{3N_0\sigma_0}{\pi m_\mu^2} \tilde{J} \sin \delta \Delta m_{21}^2 (\Delta m_{31}^2)^2 \frac{\sin^2 (AL/2)}{A^2 L^2}. \end{aligned} \quad (27)$$

We see from (27) that if we optimize $\Delta\chi^2(\text{CPV})$ with respect only to $\bar{\theta}_{13}$ then $\Delta\chi^2(\text{CPV})$ behaves as

$$\Delta\chi^2(\text{CPV}; (\delta, \theta_{13})) \simeq \frac{18N_0\sigma_0}{\pi m_\mu^2} \frac{\tilde{J}^2 \sin^2 \delta (\Delta m_{21}^2)^2 (\Delta m_{31}^2)^2 \sin^2 (AL/2)}{s_{23}^2 \sin^2 2\theta_{13} E_\mu A^2}. \quad (28)$$

Note that the behavior of $\Delta\chi^2(\text{CPV}; (\delta, \theta_{13}))$ which is optimized with respect to $\bar{\theta}_{13}$ is quite different from that of $\Delta\chi^2(\text{naive CPV})$ in (22). We observe that the dependence of $\Delta\chi^2(\text{CPV}; (\delta, \theta_{13}))$ on E_μ is the same as that of $\Delta\chi^2(\text{TV})$. It should be also emphasized that $\Delta\chi^2(\text{CPV}; (\delta, \theta_{13}))$ is proportional to $\sin^2 \delta$ and does not depend on $\cos \delta$ unlike $\Delta\chi^2(\text{naive CPV})$ in (22).

We can play the same game for θ_{23} , Δm_{32}^2 and C . In the case of the two variable correlation $(\bar{\delta}, \bar{\theta}_{23})$,

$$\sin \bar{\theta}_{23} = \sin \theta_{23} - \frac{4\tilde{J}}{s_{23} \sin^2 2\theta_{13}} \frac{\Delta m_{21}^2}{\Delta m_{31}^2} (\cos \bar{\delta} - \cos \delta) \quad (29)$$

minimizes $\Delta\chi^2(\text{CPV}; (\delta, \theta_{23}))$ and we have

$$\Delta\chi^2(\text{CPV}; (\delta, \theta_{23})) \simeq \frac{18N_0\sigma_0}{\pi m_\mu^2} \frac{\tilde{J}^2 \sin^2 \delta (\Delta m_{21}^2)^2 (\Delta m_{31}^2)^2 \sin^2 (AL/2)}{s_{23}^2 \sin^2 2\theta_{13} E_\mu A^2}, \quad (30)$$

which is the same as $\Delta\chi^2(\text{CPV}; (\delta, \theta_{13}))$. In the case of the two variable correlation $(\bar{\delta}, \Delta m_{32}^2)$, using

$$P(\nu_e \rightarrow \nu_\mu; \delta) \simeq \left[s_{23} \sin 2\theta_{13} \frac{\Delta E_{31}}{A} \sin \left(\frac{AL}{2} \right) + \frac{4\tilde{J}}{s_{23} \sin 2\theta_{13}} \frac{\Delta E_{21}}{A} \sin \left(\frac{AL}{2} \right) \cos \delta \right]^2, \quad (31)$$

we find

$$\overline{\Delta m_{31}^2} = \Delta m_{31}^2 - \frac{4\tilde{J}}{s_{23}^2 \sin^2 2\theta_{13}} \Delta m_{21}^2 (\cos \bar{\delta} - \cos \delta) \quad (32)$$

minimizes $\Delta\chi^2(\text{CPV}; (\delta, \Delta m_{31}^2))$. We obtain

$$\Delta\chi^2(\text{CPV}; (\delta, \Delta m_{31}^2)) \simeq \frac{18N_0\sigma_0}{\pi m_\mu^2} \frac{\tilde{J}^2 \sin^2 \delta (\Delta m_{21}^2)^2 (\Delta m_{31}^2)^2 \sin^2 (AL/2)}{s_{23}^2 \sin^2 2\theta_{13} E_\mu A^2}, \quad (33)$$

which again is the same as $\Delta\chi^2(\text{CPV}; (\delta, \theta_{13}))$. In the case of the two variable correlation $(\bar{\delta}, \bar{C})$,

$$\frac{\sin(\bar{A}L/2)}{\bar{A}} = \frac{\sin(AL/2)}{A} \left[1 - \frac{4\tilde{J}}{s_{23}^2 \sin^2 2\theta_{13}} \frac{\Delta m_{21}^2}{\Delta m_{31}^2} (\cos \bar{\delta} - \cos \delta) \right] \quad (34)$$

minimizes $\Delta\chi^2(\text{CPV}; (\delta, C))$ and we get

$$\Delta\chi^2(\text{CPV}; (\delta, C)) \simeq \frac{18N_0\sigma_0}{\pi m_\mu^2} \frac{\tilde{J}^2 \sin^2 \delta (\Delta m_{21}^2)^2 (\Delta m_{31}^2)^2 \sin^2 (AL/2)}{s_{23}^2 \sin^2 2\theta_{13} E_\mu A^2}, \quad (35)$$

which once again is the same as $\Delta\chi^2(\text{CPV}; (\delta, \theta_{13}))$. The expressions (25), (29), (32) and (34) for the optimal values for $\bar{\theta}_{13}$, $\bar{\theta}_{23}$, $\bar{\Delta m_{31}^2}$ and \bar{C} explain why the correlation has a cosine curve for large E_μ and small L in Figs. 1, 2, 4 and 6.

In the case of the correlations $(\bar{\delta}, \bar{\theta}_{12})$, and $(\bar{\delta}, \bar{\Delta m_{21}^2})$, we have to take into account of terms of order $\mathcal{O}((\Delta E_{21}/\Delta E_{31})^2)$. For $(\bar{\delta}, \bar{\theta}_{12})$, we have

$$\sin 2\bar{\theta}_{12} = -\frac{4\tilde{J}}{c_{23}^2} \frac{\Delta m_{31}^2}{\Delta m_{21}^2} \cos \bar{\delta} + \sqrt{\left(\frac{4\tilde{J}}{c_{23}^2} \frac{\Delta m_{31}^2}{\Delta m_{21}^2}\right)^2 \cos^2 \bar{\delta} + \frac{8\tilde{J}}{c_{23}^2} \frac{\Delta m_{31}^2}{\Delta m_{21}^2} \cos \delta \sin 2\theta_{12} + \sin^2 2\theta_{12}}, \quad (36)$$

and this optimizes $\Delta\chi^2(\text{CPV})$. We find

$$\begin{aligned} & P(\nu_e \rightarrow \nu_\mu; \theta_{12}, \delta) - P(\nu_e \rightarrow \nu_\mu; \bar{\theta}_{12}, \bar{\delta}) \\ & \simeq \frac{8\tilde{J}}{\sin 2\theta_{12}} \frac{\Delta E_{21} \Delta E_{31}}{A^2} \sin^2 \left(\frac{AL}{2} \right) \left[\sin 2\theta_{12} \cos \left(\delta + \frac{\Delta E_{31} L}{2} \right) \right. \\ & \quad \left. - \sin 2\bar{\theta}_{12} \cos \left(\bar{\delta} + \frac{\Delta E_{31} L}{2} \right) - \sin 2\theta_{12} \cos \delta + \sin 2\bar{\theta}_{12} \cos \bar{\delta} \right] \\ & \simeq \frac{8\tilde{J}}{\sin 2\theta_{12}} \frac{\Delta E_{21} \Delta E_{31}}{A^2} \sin^2 \left(\frac{AL}{2} \right) (\sin \bar{\delta} \sin 2\bar{\theta}_{12} - \sin \delta \sin 2\theta_{12}) \frac{\Delta E_{31} L}{2}, \end{aligned} \quad (37)$$

where we have expanded $\sin(\Delta E_{31} L/2) \simeq \Delta E_{31} L/2$. By putting $\bar{\delta} = 0$, we obtain

$$\Delta\chi^2(\text{CPV}; (\delta, \theta_{12})) \simeq \frac{18N_0\sigma_0}{\pi m_\mu^2} \frac{\tilde{J}^2 \sin^2 \delta (\Delta m_{21}^2)^2 (\Delta m_{31}^2)^2 \sin^2 (AL/2)}{s_{23}^2 \sin^2 2\theta_{13} E_\mu A^2}, \quad (38)$$

which once again is the same as $\Delta\chi^2(\text{CPV}; (\delta, \theta_{13}))$. For $(\bar{\delta}, \bar{\Delta m_{21}^2})$, we have

$$\begin{aligned} \bar{\Delta m_{21}^2} &= -\frac{4\tilde{J}}{c_{23}^2 \sin^2 2\theta_{12}} \Delta m_{31}^2 \cos \bar{\delta} \\ &+ \sqrt{\left(\frac{4\tilde{J}}{c_{23}^2 \sin^2 2\theta_{12}}\right)^2 \cos^2 \bar{\delta} (\Delta m_{31}^2)^2 + \frac{8\tilde{J}}{c_{23}^2 \sin^2 2\theta_{12}} \Delta m_{21}^2 \Delta m_{31}^2 \cos \delta + (\Delta m_{21}^2)^2} \end{aligned} \quad (39)$$

which leads to

$$\begin{aligned} & P(\nu_e \rightarrow \nu_\mu; \Delta m_{21}^2, \delta) - P(\nu_e \rightarrow \nu_\mu; \bar{\Delta m_{21}^2}, \bar{\delta}) \\ & \simeq 8\tilde{J} \frac{\Delta E_{21} \Delta E_{31}}{A^2} \sin^2 \left(\frac{AL}{2} \right) (\sin \bar{\delta} - \sin \delta) \frac{\Delta E_{31} L}{2}. \end{aligned} \quad (40)$$

Thus we get

$$\Delta\chi^2(\text{CPV}; (\delta, \Delta m_{21}^2)) \simeq \frac{18N_0\sigma_0}{\pi m_\mu^2} \frac{\tilde{J}^2 \sin^2 \delta (\Delta m_{21}^2)^2 (\Delta m_{31}^2)^2 \sin^2 (AL/2)}{s_{23}^2 \sin^2 2\theta_{13}} \frac{1}{E_\mu A^2}, \quad (41)$$

which once again is the same as $\Delta\chi^2(\text{CPV}; (\delta, \theta_{13}))$. Unlike the cases for $(\bar{\delta}, \bar{\theta}_{13})$, $(\bar{\delta}, \bar{\theta}_{23})$, $(\bar{\delta}, \bar{\Delta m_{31}^2})$ and $(\bar{\delta}, \bar{C})$, the optimal values (36) and (39) have nontrivial behaviors even for large E_μ and small L , as we can see from Figs. 3 and 5.

We have seen analytically that two variable correlations give us the behavior $\Delta\chi^2(\text{CPV}) \propto \sin^2 \delta / E_\mu$ and this behavior is the same as $\Delta\chi^2(\text{TV})$. Although it is difficult to discuss correlations of more than two variables analytically, the discussions above are sufficient to demonstrate that sensitivity to CP violation decreases as E_μ becomes larger. In fact we have verified numerically that $\Delta\chi^2(\text{CPV})$ decreases as the muon energy increases ($E_\mu \gtrsim 100\text{GeV}$). The conclusion in this subsection is qualitatively consistent with the work [36] by Lipari who claims that sensitivity to CP violation decreases as E_μ becomes large. However it may not be quantitatively consistent with [36] in which it was suggested that sensitivity starts getting lost for $E_\nu \gtrsim$ a few GeV. In our discussion here it was necessary to have $|\Delta E_{31}L| \ll 1$ which may not be attained for $L \sim 3000\text{km}$ and $E_\mu \lesssim 50\text{GeV}$. Our numerical calculations in the previous section indicate that the sensitivity is optimized for $20\text{GeV} \lesssim E_\mu \lesssim 50\text{GeV}$ which is quantitatively consistent with the results in [21–31]. This interval for E_μ is the intermediate energy region which cannot be treated analytically using our arguments in this section. In fact it seems difficult to explain analytically the strong correlation of $(\bar{\delta}, \bar{C})$ for $E_\mu \simeq 50\text{ GeV}$ and $L \simeq 3000\text{km}$. (cf. Fig. 1)

V. JHF EXPERIMENT

The JHF project [18] has been proposed to perform precise measurements of the oscillation parameters. The possible extension of this project includes the upgrade of the power to 4MW and the construction of a mega-ton detector [39]. The possibility to measure CP violation at the JHF project has been discussed by [45,42,46]. Here we briefly discuss the possibility of measurements of CP violation at the JHF experiment with power 4MW and a 1 Mton detector as a comparison with neutrino factories. As in previous sections, we will take into consideration the correlations of all the oscillation parameters. In the case of the JHF experiment, which has the baseline $L \simeq 300\text{km}$, the matter effect is almost negligible and it is possible to compare the numbers of events for $\nu_\mu \rightarrow \nu_e$ and $\bar{\nu}_\mu \rightarrow \bar{\nu}_e$ directly by taking into account the difference of the cross sections between $\sigma_{\nu N}$ and $\sigma_{\bar{\nu} N}$. However, we use the same $\Delta\chi^2$ as in section 2, as discussions with the same criterion gives more transparent comparisons between neutrino factories and the superbeam at JHF.

The correlations of two variables (δ, X) , where X is $\theta_{k\ell}$, $\Delta m_{k\ell}^2$ or C , are shown in Fig. 11, where the central values for these parameters are those of the best fit point, i.e., $\sin^2 2\theta_{12} = 0.75$, $\Delta m_{21}^2 = 3.2 \times 10^{-5}\text{eV}^2$; $\sin^2 2\theta_{23} = 1.0$, $\Delta m_{32}^2 = 3.2 \times 10^{-3}\text{eV}^2$, $C=1.0$ and we have used a reference value $\theta_{13} = 8^\circ$. In this calculation the narrow band beam (NBB) (the flux referred to as LE2 π in [18]) is used, and it is assumed for simplicity that there are no backgrounds and the detection efficiency is 70% in Fig. 11. Note that for the purpose of measurements of CP violation NBB is more advantageous than the wide band beam, as the former has better energy resolution.

As in the section 2, we have evaluated numerically the data size required to reject a hypothesis with $\bar{\delta} = 0$. Of course the data size depends on the true value δ and the results obtained by varying the six variables $(\theta_{k\ell}, \Delta m_{k\ell}^2, C)$ are plotted in Fig. 12, where we have taken the best fit values for $(\theta_{12}, \Delta m_{21}^2)$, $(\theta_{23}, \Delta m_{32}^2)$, $\theta_{13} = 8^\circ, 5^\circ, 1^\circ (2^\circ)$, and the NBB is used. The vertical axis of Fig. 12 stands for the data size required per $\text{kt} \times (\nu_\mu \text{ 1 year} + \bar{\nu}_\mu \text{ 2 years})$. We have used two ways of ν_e selections, one is 1-ring e-like selection which has the background fraction $f_B = 1.8 \times 10^{-2}$, the detection efficiency 70.4%, and the other one is π^0 cut selection which has the background fraction $f_B = 2 \times 10^{-3}$, the detection efficiency 50.4% [45]. In the case of the 1-ring e-like selection, for $\theta_{13} = 1^\circ$ the systematic error becomes so large that the data size required to reject $\delta = 0$ becomes infinite. Also in this case the number of events for $\delta = \pi$ becomes almost the same as that for $\delta = 0$ up to the systematic errors and there is no way to distinguish the case of $\delta = \pi$ and that of $\delta = 0$. However, as long as the value of δ is not close to 0 or π and $\theta_{13} \gtrsim 3^\circ$, the JHF with 4MW power and a 1 mega ton detector will be able to demonstrate $\delta \neq 0$ at $3\sigma\text{CL}$.

VI. DISCUSSIONS

In order to be more concrete, we need the knowledge on the uncertainty of the matter effect A . The error of $A = \sqrt{2}G_F Y_e \rho$ comes from those of Y_e and ρ . The error of Y_e has been discussed by [47] and it is about 2% and geophysicists [48,49] agree with it. Without any uncertainty of the matter effect, it has been claimed that a medium baseline experiment ($L \sim 3000\text{km}$, $E_\mu \sim 50\text{GeV}$) is best for measurements of CP violation. In that case the depth of the neutrino path is at most 200km and most of the neutrino path is in the upper mantle. It is known in geophysics [50] that the crust has relatively large latitude-longitude dependent fluctuations around constant density. On the other hand, in the case of the upper mantle, some geophysicists claim that fluctuations around constant density are a few % [51,48,49] while another [52] says that they may be as large as 5 %. However, such discussions are based on normal mode studies in seismology which are confined to long wavelength features, and it was pointed out [49,52] that the fluctuations in the density in the analysis of neutrino factories may be larger than 5 %, since the width of the neutrino beam is much smaller than typical wavelengths in seismological studies. If that is the case, then it follows from Fig. 8 that the case $L \simeq 1000\text{km}$ is better than the case $L \simeq 3000\text{km}$, since the former is insensitive to the uncertainty of the matter effect. More detailed analysis with seismological discussions seems to be necessary to determine the optimal baseline and the muon energy in neutrino factories.

We have also seen that if there is a nontrivial fraction of backgrounds, which is expected in the case of water Cherenkov or liquid argon detectors, then medium energy ($10\text{GeV} \lesssim E_\mu \lesssim 20\text{GeV}$) is more advantageous than high energy ($E_\mu \sim 50\text{GeV}$), as systematic errors become so large in the latter case.

The bottom line of the present paper is that either the high or medium energy option is certainly better than the low energy option which has been advocated by some people [32,34]. We have arrived at this conclusion on the assumption that the energy threshold is as low as 0.1 GeV, and the detection efficiency is independent of the neutrino energy. In practice, it may be very difficult to have such a low threshold and to keep such a good detection efficiency down to 0.1 GeV, so it is expected that the low energy option ($E_\nu \lesssim$

10GeV) becomes less and less advantageous.

If we can realize a nearly perfectly polarized muon beam, it may be possible to measure T violation, which is much better than CP violation, since we do not have to worry about the uncertainty of the density of the Earth or other oscillation parameters and a nonzero value of T violation immediately indicates $\delta \neq 0$. Efforts should be made along these lines.

If $\theta_{13} \gtrsim 3^\circ$ and if the value of δ is not close to 0 or π , then the JHF experiment with 4MW power and a 1 mega ton detector will be able to demonstrate $\delta \neq 0$ at 3σ CL. On the other hand, if $\theta_{13} \lesssim 3^\circ$, then neutrino factories seem to be the only experiment which can demonstrate $\delta \neq 0$. In that case, depending on the situation such as the fraction of backgrounds, the uncertainty of the matter effect and the magnitude of θ_{13} , the option with ($E_\mu \simeq 50\text{GeV}$, $L \simeq 3000\text{km}$) may be advantageous (or disadvantageous) over ($E_\mu \simeq 20\text{GeV}$, $L \simeq 1000\text{km}$). In both a neutrino factory with ($20\text{GeV} \lesssim E_\mu \lesssim 50\text{GeV}$, $1000\text{km} \lesssim L \lesssim 3000\text{km}$) and the JHF experiment, our $\Delta\chi^2(\text{CPV})$ depends not only on $\sin \delta$ but also $\cos \delta$,⁴ so that we can in principle distinguish $\delta = \pi$ from $\delta = 0$ as long as the statistical significance overcomes the systematic errors. This is not the case for a neutrino factory with large systematic errors for small θ_{13} , i.e., for $E_\mu = 50\text{GeV}$ and $\theta_{13} = 1^\circ$ (cf. Fig. 9), and for the JHF experiment with less S/N ratio i.e., when the 1-ring e-like selection is adopted, or when $\theta_{13} = 8^\circ$ and the π^0 cut selection is adopted (cf. Fig. 12).

In this paper we adopted simplified assumptions such as that the detection efficiency is independent of the neutrino energy, that the threshold energy can be taken as low as 0.1GeV, and that the uncertainty of the matter effect is at most 5 %, but we need much more detailed experimental information to obtain the optimum muon energy and the baseline.

NOTE ADDED

Just before we hit a return key to submit our paper to the preprint archive, we became aware of the work by M. Freund et al. [53], where the similar topics has been discussed from a slightly different viewpoint.

ACKNOWLEDGMENTS

O. Y. would like to thank R. Geller, Y. Fukao and H. Yamazaki for discussions on the density of the Earth, J. Resovsky, M. Ishii, C. Kuo, D.L. Anderson, T. Tanimoto and J. Tromp for useful communications on the uncertainty of the density of the Earth, and Y. Kuno and Y. Mori for discussions on neutrino factories. We thank Kenji Ogawa for his contribution in the earlier stage of this work, P. Lipari, H. Minakata and H. Nunokawa for discussions. This research was supported in part by a Grant-in-Aid for Scientific Research of the Ministry of Education, Science and Culture, #12047222, #13640295.

⁴If we evaluate $\Delta\chi^2(\text{CPV}; (\delta, \theta_{13}))$ in (28) to the next leading order in $\Delta m_{31}^2 L/E_\mu$ then $\tilde{J}^2 \sin^2 \delta$ in (28) is replaced by $\tilde{J}^2 (\sin \delta + \text{const.} (\Delta m_{31}^2 L/E_\mu \cos \delta)^2)$, and $\Delta m_{31}^2 L/E_\mu$ is not necessarily negligible in either case.

REFERENCES

- [1] B.T. Cleveland et al., Nucl. Phys. B (Proc. Suppl.) **38** (1995) 47.
- [2] Y. Fukuda et al., Phys. Rev. Lett. **77** (1996) 1683 and references therein.
- [3] Y. Suzuki, Nucl. Phys. B (Proc. Suppl.) **77** (1999) 35 and references therein.
- [4] V.N. Gavrin, Nucl. Phys. B (Proc. Suppl.) **77** (1999) 20 and references therein.
- [5] T.A. Kirsten, Nucl. Phys. B (Proc. Suppl.) **77** (1999) 26 and references therein.
- [6] Y. Fukuda et al., Phys. Lett. **B335** (1994) 237 and references therein.
- [7] R. Becker-Szendy et al., Phys. Rev. **D46** (1992) 3720 and references therein.
- [8] T. Kajita and Y. Totsuka, Rev. Mod. Phys. **73**, 85 (2001) and references therein; J.G. Learned, hep-ex/0007056.
- [9] Y. Fukuda et al., Phys. Rev. Lett. **82** (1999) 2644.
- [10] W.W.M. Allison et al., Phys. Lett. **B449** (1999) 137.
- [11] C. Athanassopoulos *et al.*, (LSND Collaboration), Phys. Rev. Lett. **77**, 3082 (1996); Phys. Rev. **C54**, 2685 (1996); Phys. Rev. Lett. **81**, 1774 (1998); Phys. Rev. **C58**, 2489 (1998); D.H. White, Nucl. Phys. Proc. Suppl. **77** 207 (1999).
- [12] Z. Maki, M. Nakagawa and S. Sakata, Prog. Theor. Phys. **28** (1962) 870.
- [13] O. Yasuda, Acta Phys. Pol. **B30** (1999) 3089.
- [14] M.C. Gonzalez-Garcia, M. Maltoni, C. Pena-Garay, J.W.F. Valle, Phys. Rev. **D63**, 033005 (2001).
- [15] G.L. Fogli, E. Lisi, A. Marrone, D. Montanino and A. Palazzo, hep-ph/0104221.
- [16] M. Apollonio *et al.*, Phys. Lett. B **338** (1998) 383; Phys. Lett. B **466**, 415 (1999).
- [17] MINOS experiment, <http://www.hep.anl.gov/NDK/HyperText/numi.html>
- [18] Y. Itow et al., Letter of Intent, http://www-jhf.kek.jp/JHF_WWW/LOI/jhfnu_loi.ps.
- [19] S. Geer, Phys. Rev. **D57**, 6989 (1998), erratum *ibid.* **D59** (1999) 039903.
- [20] B. Autin et al., CERN-SPSC-98-30; A. De Rujula, M.B. Gavela and P. Hernandez, Nucl. Phys. **B547** (1999) 21; S. Dutta, R. Gandhi and B. Mukhopadhyaya, hep-ph/9905475; V. Barger, S. Geer and K. Whisnant, Phys. Rev. **D61** (2000) 053004; M. Tanimoto, Phys. Lett. **B462** (1999) 115; A. Kalliomaki, J. Maalampi and M. Tanimoto, Phys. Lett. **B469** (1999) 179; A. Romanino, hep-ph/9909425; M. Koike and J. Sato, Phys. Rev. **D61** (2000) 073012; A. Donini, M.B. Gavela, P. Hernandez and S. Rigolin, hep-ph/9909254; hep-ph/9910516; V. Barger, S. Geer, R. Raja and K. Whisnant, hep-ph/9911524; D. Ayres et al., physics/9911009.
- [21] V. Barger, S. Geer and K. Whisnant, Phys. Rev. **D61** (2000) 053004.
- [22] A. Cervera, A. Donini, M.B. Gavela, J. J. Gomez Cadenas, P. Hernandez, O. Mena and S. Rigolin, Nucl. Phys. **B579** (2000) 17.
- [23] V. Barger, S. Geer, R. Raja and K. Whisnant, Phys. Rev. **D62** (2000) 013004; Phys. Lett. **B485** (2000) 379; hep-ph/0007181.
- [24] V. Barger, S. Geer, R. Raja and K. Whisnant, Phys. Rev. **D62** (2000) 073002;
- [25] A. De Rujula, M. B. Gavela and P. Hernandez, Nucl. Phys. **B547**, 21 (1999); A. Donini, M. B. Gavela, P. Hernandez and S. Rigolin, Nucl. Phys. **B574** (2000) 23.
- [26] K. Dick, M. Freund, M. Lindner, and A. Romanino, Nucl. Phys. **B562** (1999) 29; A. Romanino, Nucl. Phys. **B574** (2000) 675; M. Freund, P. Huber and M. Lindner, Nucl. Phys. **B585** (2000) 105.
- [27] M. Freund, M. Lindner, S.T. Petcov and A. Romanino, Nucl. Phys. **B578** (2000) 27.

- [28] Neutrino Factory and Muon Collider Collaboration (D. Ayres *et al.*), physics /9911009; C. Albright *et al.* hep-ex/0008064.
- [29] M. Campanelli, A. Bueno and A. Rubbia, hep-ph/9905240; A. Bueno, M. Campanelli and A. Rubbia, Nucl. Phys. **B573** (2000) 27; Nucl. Phys. **B589** (2000) 577.
- [30] J. Sato, hep-ph/0006127; M. Koike and J.Sato, Phys. Rev. **D61** (2000) 073012.
- [31] O. Yasuda, hep-ph/0005134.
- [32] J. Sato, talk at International Workshop on Muon Storage Ring for a Neutrino Factory (NUFACT'00), Monterey, California, 22 – 26 May 2000; talk at the Joint U.S./Japan Workshop On New Initiatives In Muon Lepton Flavor Violation and Neutrino Oscillation With High Intense Muon and Neutrino Sources, Honolulu, Hawaii, Oct. 2–6, 2000; talk at JSPS-KOSEF Joint Workshop on "New Developments in Neutrino Physics", Korea Institute for Advanced Study, Seoul, Korea, 16 - 20 October 2000; hep-ph/0008056; T. Ohta and J. Sato, hep-ph/0011234; M. Koike, T. Ohta and J.Sato, hep-ph/0011387.
- [33] T. Miura, E. Takasugi, Y. Kuno, M. Yoshimura, hep-ph/0102111.
- [34] H. Minakata and H. Nunokawa, Phys. Lett. **B495**, 369 (2000).
- [35] B. Richter, hep-ph/0008222.
- [36] P. Lipari, hep-ph/0102046.
- [37] M. Nakahata et. al., J. Phys. Soc. Japan, **55** (1986) 3786.
- [38] P. Lipari, M. Lusignoli and F. Sartogo, Phys. Rev. Lett. **74**, 4384 (1995).
- [39] K. Nakamura, talk at the Joint U.S./Japan Workshop On New Initiatives In Muon Lepton Flavor Violation and Neutrino Oscillation With High Intense Muon and Neutrino Sources, Honolulu, Hawaii, Oct. 2–6, 2000, http://meco.ps.uci.edu/lepton_workshop/talks/nakamura.pdf.
- [40] D. Casper, talk at Joint U.S. / Japan Workshop on New Initiatives in Lepton Flavor Violation and Neutrino Oscillation with High Intense Muon and Neutrino Sources, Honolulu, Hawaii, 2-6 Oct 2000, http://meco.ps.uci.edu/lepton_workshop/talks/casper/uno.pdf.
- [41] F. Stacey, *Physics of the Earth*, 2nd ed. (J. Wiley and Sons, Chichester, 1977).
- [42] V. Barger, S. Geer, R. Raja and K. Whisnant, hep-ph/0012017.
- [43] M.C. Gonzalez-Garcia and C. Pena-Garay, hep-ph/0009041.
- [44] J. Burguet-Castell, M.B. Gavela, J.J. Gomez-Cadenas, P. Hernandez, O. Mena, hep-ph/0103258.
- [45] Y. Obayashi, talk at the Joint U.S./Japan Workshop On New Initiatives In Muon Lepton Flavor Violation and Neutrino Oscillation With High Intense Muon and Neutrino Sources, Honolulu, Hawaii, Oct. 2–6, 2000, http://meco.ps.uci.edu/lepton_workshop/talks/obayashi.pdf.
- [46] T. Kobayashi, talk at the 5th Tokutei-RCCN Workshop on Neutrinos, ICRR, Univ. of Tokyo, Kashiwa, Japan, Feb. 23–24, 2001.
- [47] M. Maris and S.T. Petcov Phys. Rev. **D56**, 7444 (1997).
- [48] D.L. Anderson, private communication.
- [49] T. Tanimoto, private communication.
- [50] T. Tanimoto, J. Phys. Earth **38**, 493 (1990).
- [51] J. Resovsky, private communication.
- [52] R. Geller, private communication.
- [53] M. Freund, P. Huber and M. Lindner, hep-ph/0105071.

Figures

Fig.1a Correlations of errors of $\bar{\delta}$ and the normalization \bar{C} for $L=100\text{km}$, 1000km , 2500km , 6300km and for $E_\mu=3\text{GeV}$, 20GeV , 50GeV . $\Delta\chi^2 = 0.18, 0.37, 0.73$ corresponds to $1\sigma\text{CL}$, $90\%\text{CL}$, $99\%\text{CL}$, respectively for two degrees of freedom. The oscillation parameters are $\Delta m_{21}^2 = 1.8 \times 10^{-5}\text{eV}^2$, $\Delta m_{32}^2 = 3.5 \times 10^{-5}\text{eV}^2$, $\sin^2 2\theta_{12} = 0.76$, $\sin^2 2\theta_{23} = 1.0$, $\theta_{13} = 8^\circ$, $\delta = \pi/2$. The number of useful muon decays is $10^{21}\mu \cdot 10\text{kt}$. No backgrounds are taken into consideration in Figs. 1–6.

Fig.1b The same correlation as Fig.1a for $\theta_{13} = 5^\circ$, 1° . The oscillation parameters and other reference values are the same as in Fig. 1a.

Fig.2 Correlations of errors of $\bar{\delta}$ and $\bar{\theta}_{13}$. The oscillation parameters and other reference values are the same as in Fig. 1a.

Fig.3 Correlations of errors of $\bar{\delta}$ and $\bar{\theta}_{12}$. The oscillation parameters and other reference values are the same as in Fig. 1a.

Fig.4 Correlations of errors of $\bar{\delta}$ and $\bar{\theta}_{23}$. The oscillation parameters and other reference values are the same as in Fig. 1a.

Fig.5 Correlations of errors of $\bar{\delta}$ and $\overline{\Delta m_{21}^2}$. The oscillation parameters and other reference values are the same as in Fig. 1a.

Fig.6 Correlations of errors of $\bar{\delta}$ and $\overline{\Delta m_{32}^2}$. The oscillation parameters and other reference values are the same as in Fig. 1a.

Fig.7 The contour plot of equi-number of data size required (in the unit of kt) to reject a hypothesis $\bar{\delta} = 0$ at 3σ using $\Delta\chi^2(\text{CPV})$ (3) in the case of a neutrino factory with 10^{21} useful muon decays, the background fraction $f_B = 10^{-5}$ or 10^{-3} , $\theta_{13} = 8^\circ$, 5° , 1° . The other oscillation parameters are the same as in Fig. 1.

Fig.8 The same as Fig.7 with $\theta_{13} = 8^\circ$, except that the uncertainty of the matter effect is assumed to be larger $|\Delta C| \leq 0.1$ or $|\Delta C| \leq 0.2$.

Fig.9 The number of data size required to reject a hypothesis $\bar{\delta} = 0$ at 3σ for a neutrino factory using $\Delta\chi^2(\text{CPV})$ (3) as a function of the true value of δ for $f_B = 10^{-3}$. All the assumptions except for δ are the same as in Fig. 7. The situation is improved for smaller θ_{13} .

Fig.10 The contour plot of equi-number of data size required (in the unit of kt) to reject a hypothesis $\bar{\delta} = 0$ at 3σ using T violation (5) in the case of a neutrino factory with 10^{21} useful muon decays, the background fraction $f_B = 10^{-5}$ or 10^{-3} , $\theta_{13} = 8^\circ$, 5° , 1° . The other oscillation parameters are the same as in Fig. 1. Crucial assumption in this case is that the polarization is perfect, and under this assumption T violation is 3 times better than the CP violation analysis in section 2.

Fig.11 The correlations of errors of $(\bar{\delta}, \bar{C})$, $(\delta, \bar{\theta}_{13})$, $(\delta, \bar{\theta}_{12})$, $(\delta, \bar{\theta}_{23})$, $(\delta, \overline{\Delta m_{21}^2})$, $(\delta, \overline{\Delta m_{32}^2})$ in the case of the JHF experiment with 4MW power, a 1 mega ton detector and NBB. No backgrounds are taken into consideration in these figures. The oscillation parameters used are the same as in Fig. 1.

Fig.12 The number of data size required (in the unit of kt) to reject a hypothesis $\bar{\delta} = 0$ at 3σ for the JHF experiment with 4MW power, a 1 mega ton detector and NBB using $\Delta\chi^2(\text{CPV})$ (3) as a function of the true value of δ . Unlike in the case of Fig.11, the effects of backgrounds are taken into account in this figure. The oscillation parameters used are the same as in Fig. 1, and two ways of cuts (1-ring e-like and π^0 cut) [45] are used. In the case of the 1-ring e-like selection, $\theta_{13} = 1^\circ$ does not have a solution because the systematic errors become so large.

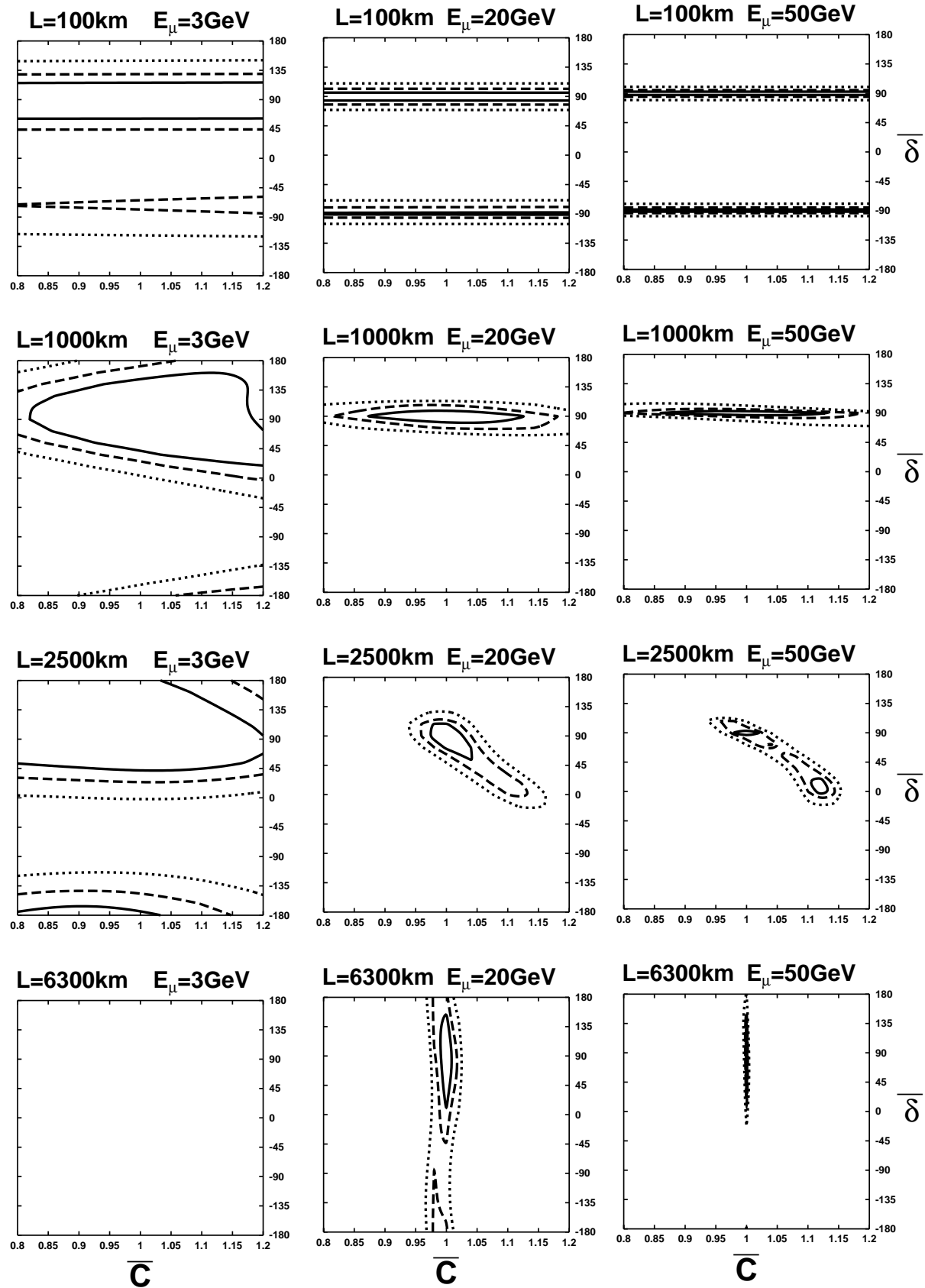
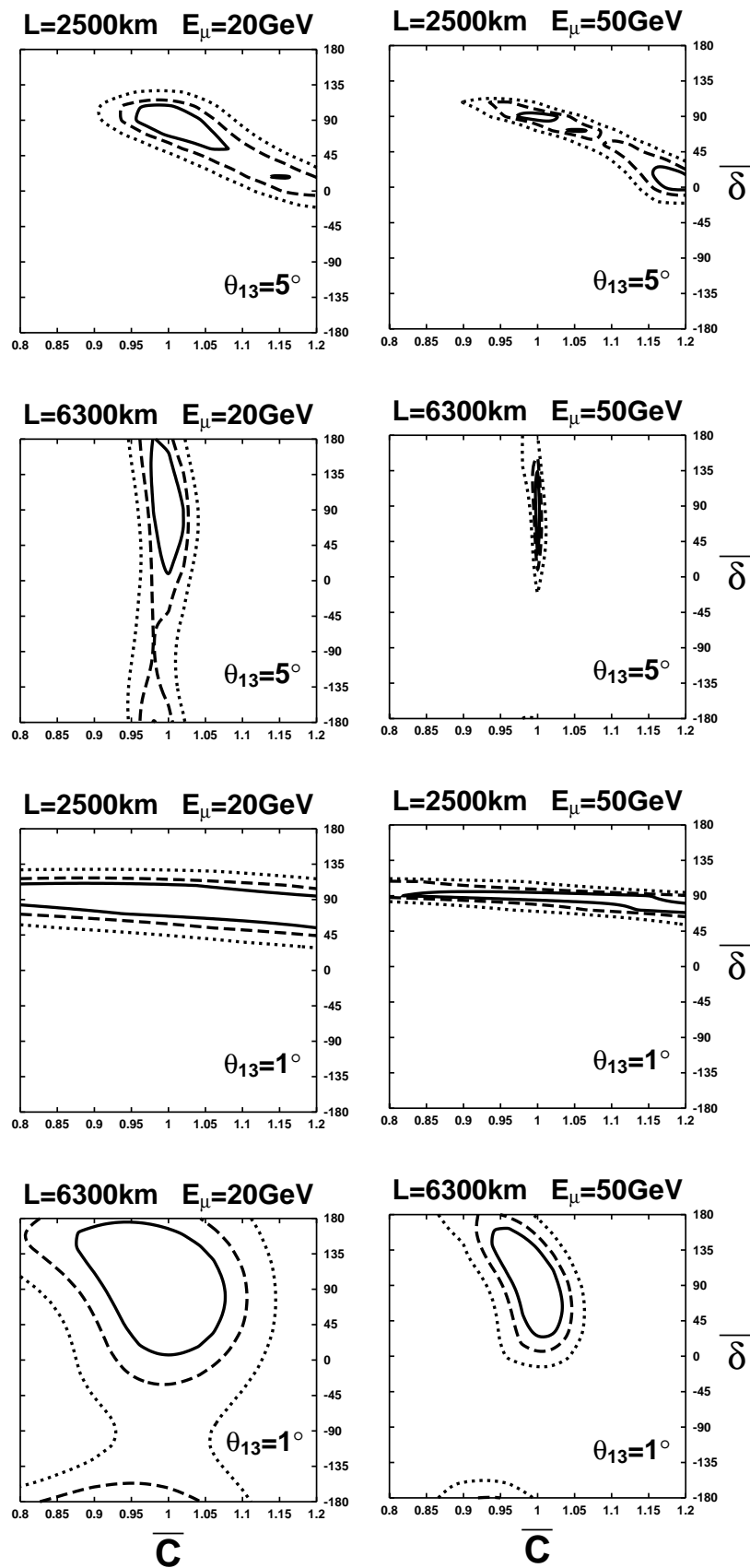
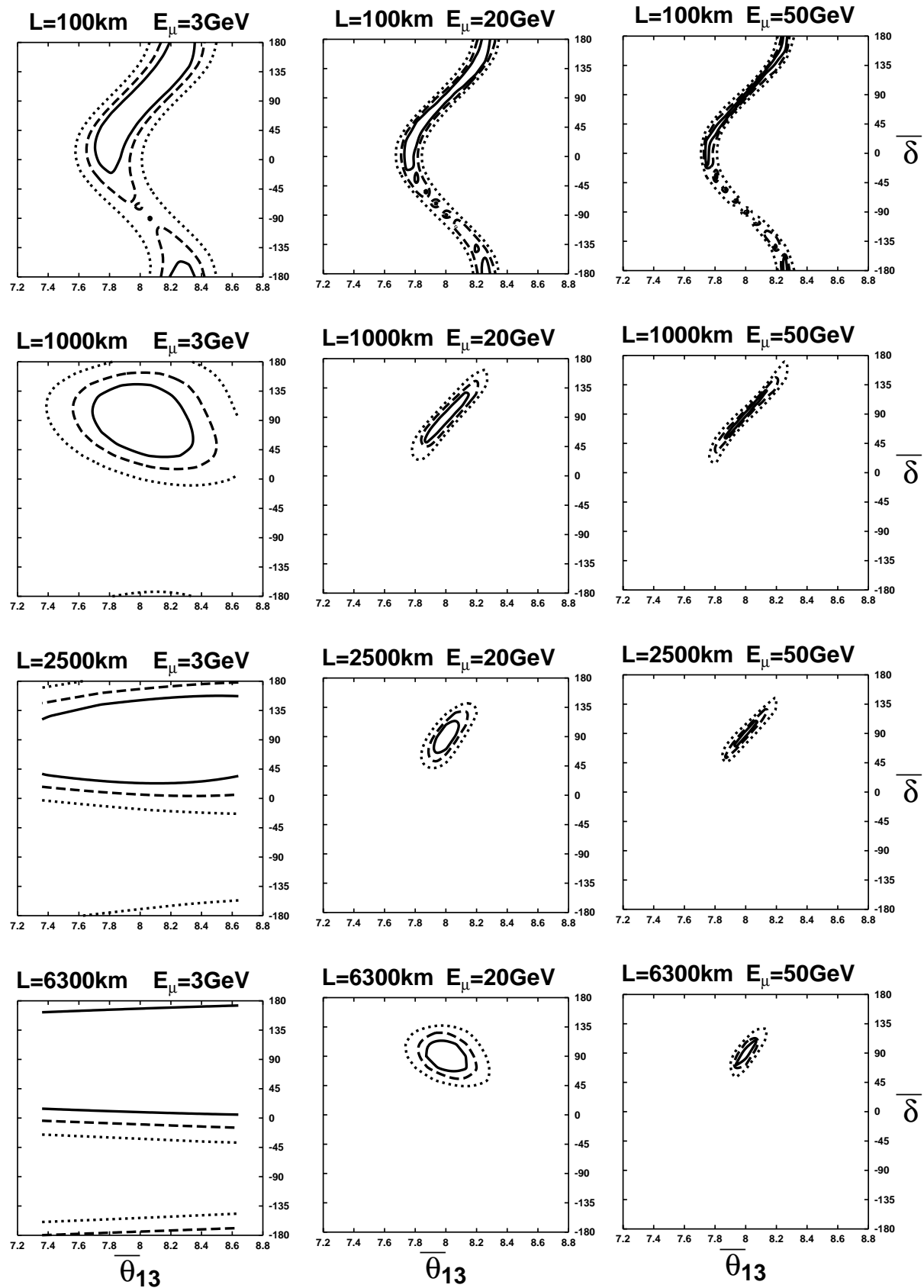


Fig.1a



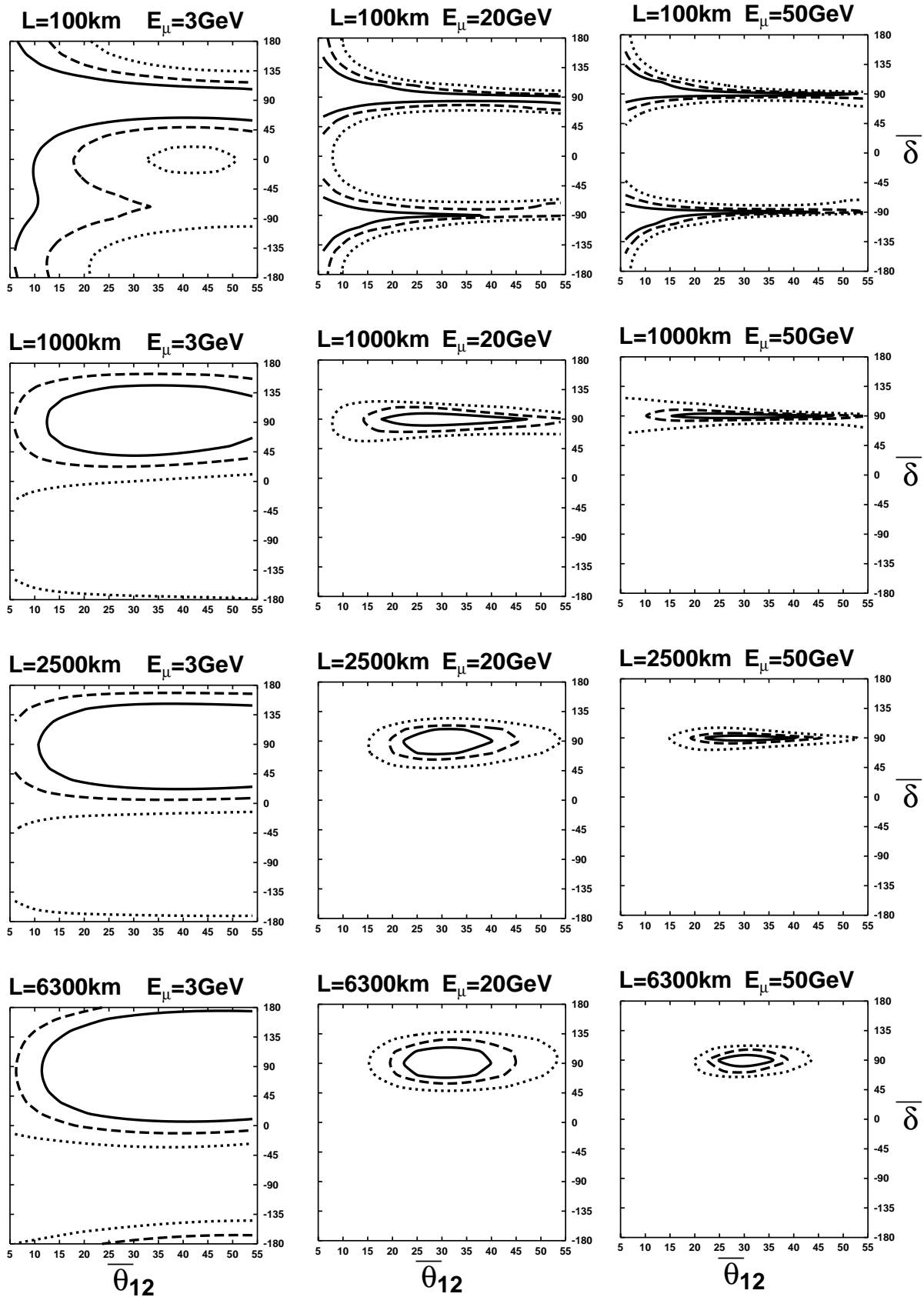
68%CL —
 90%CL - - -
 99%CL

Fig.1b



68%CL —
 90%CL - -
 99%CL

Fig.2



68%CL —
 90%CL - -
 99%CL

Fig.3

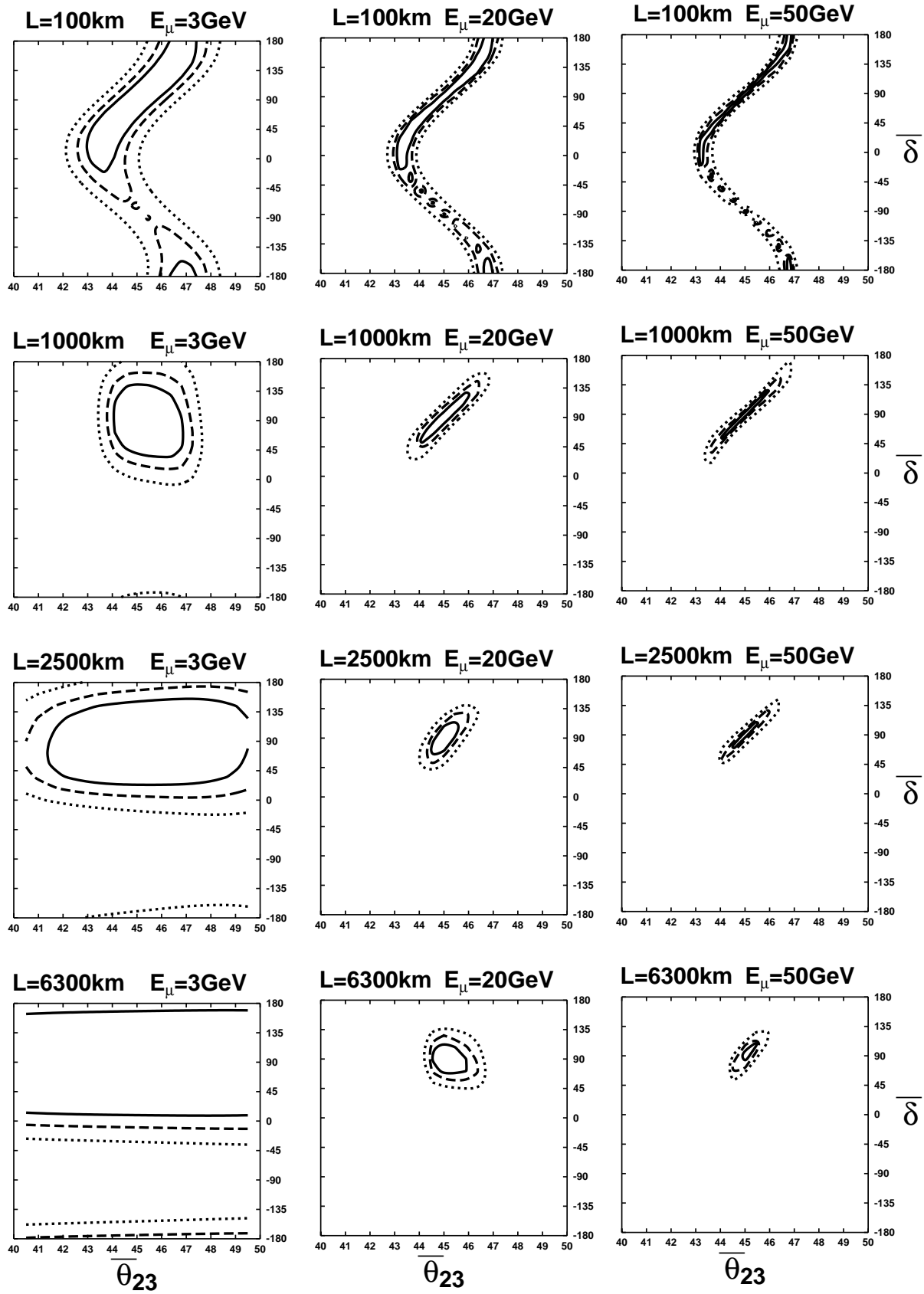


Fig.4

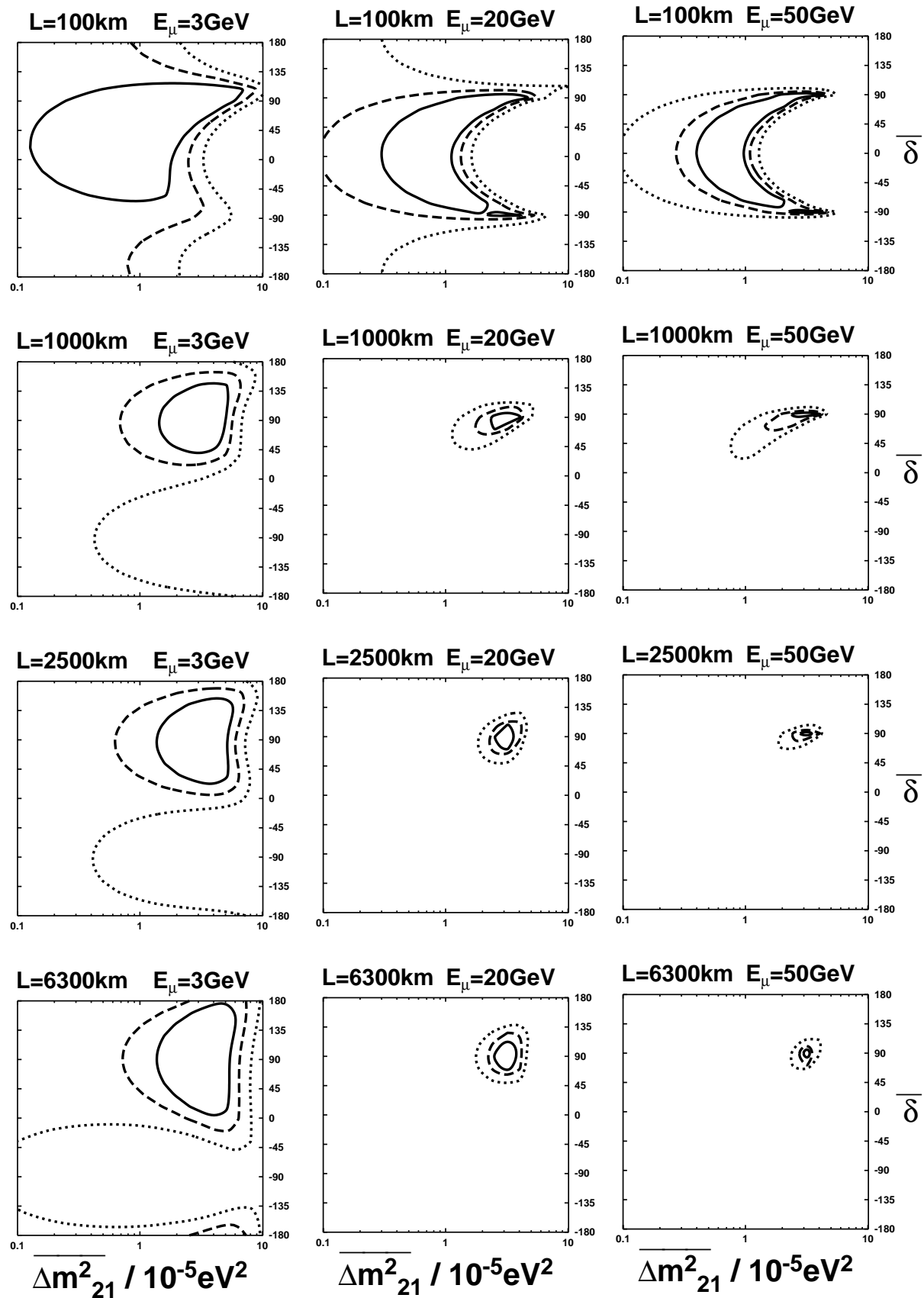
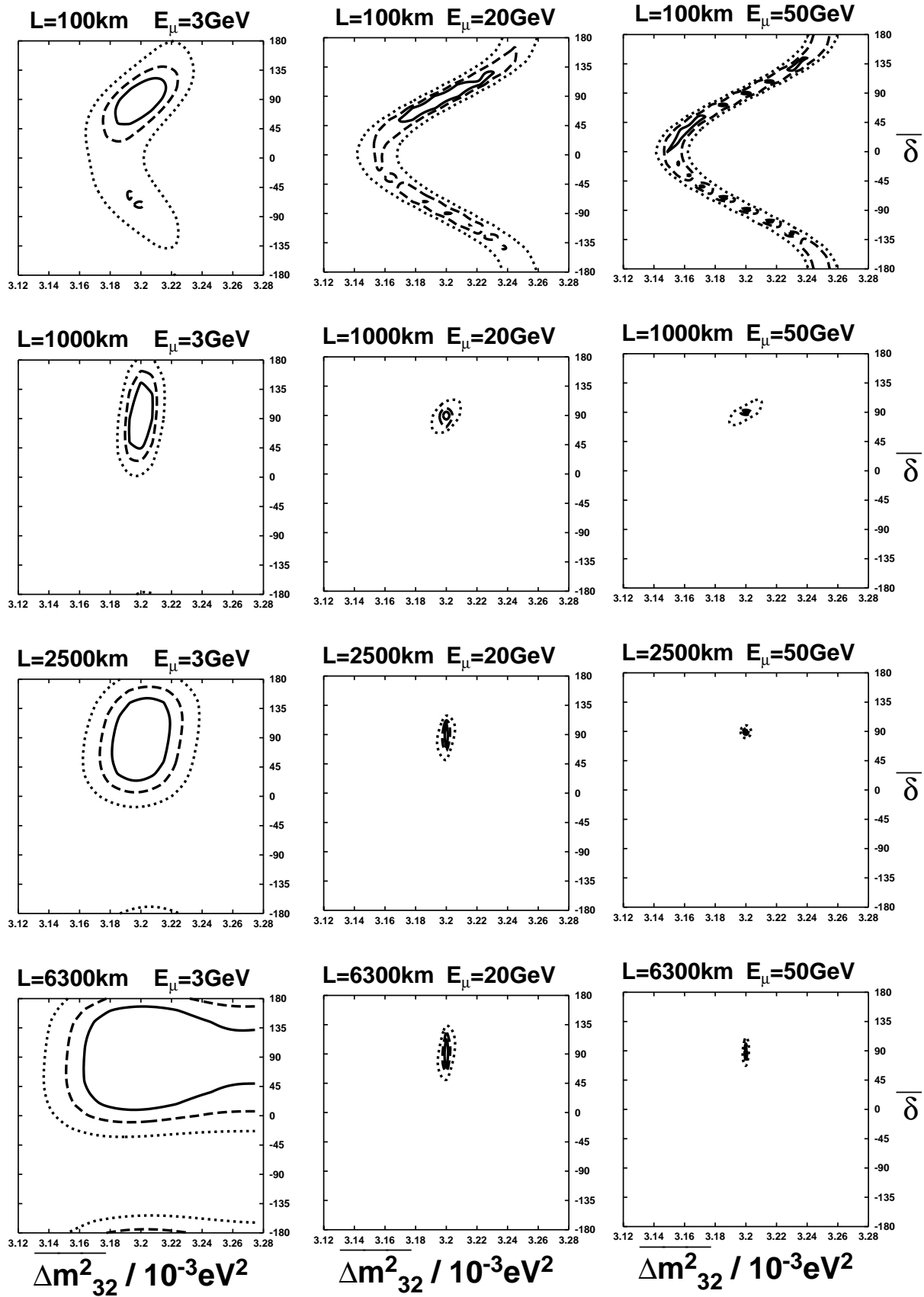
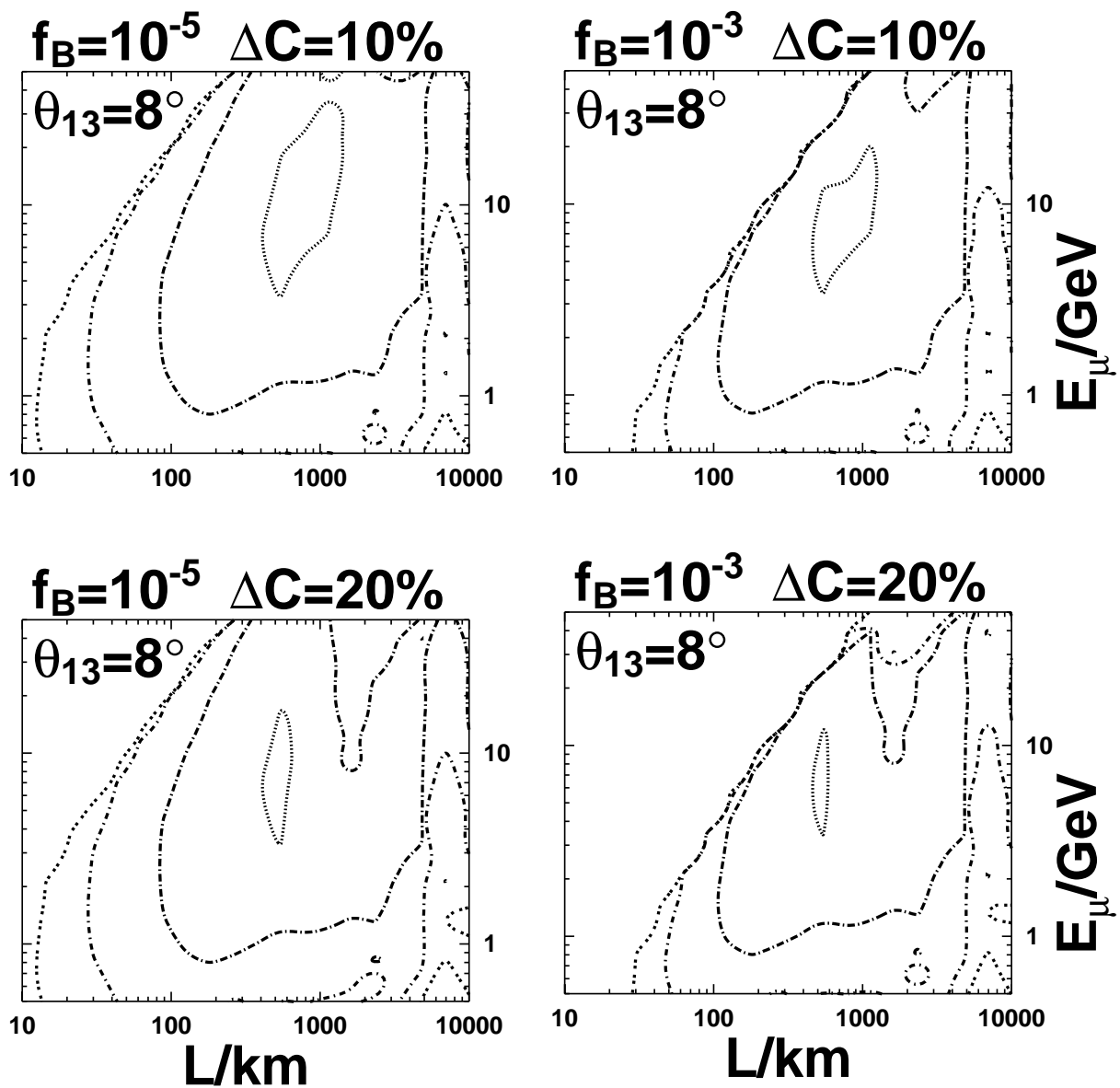


Fig.5



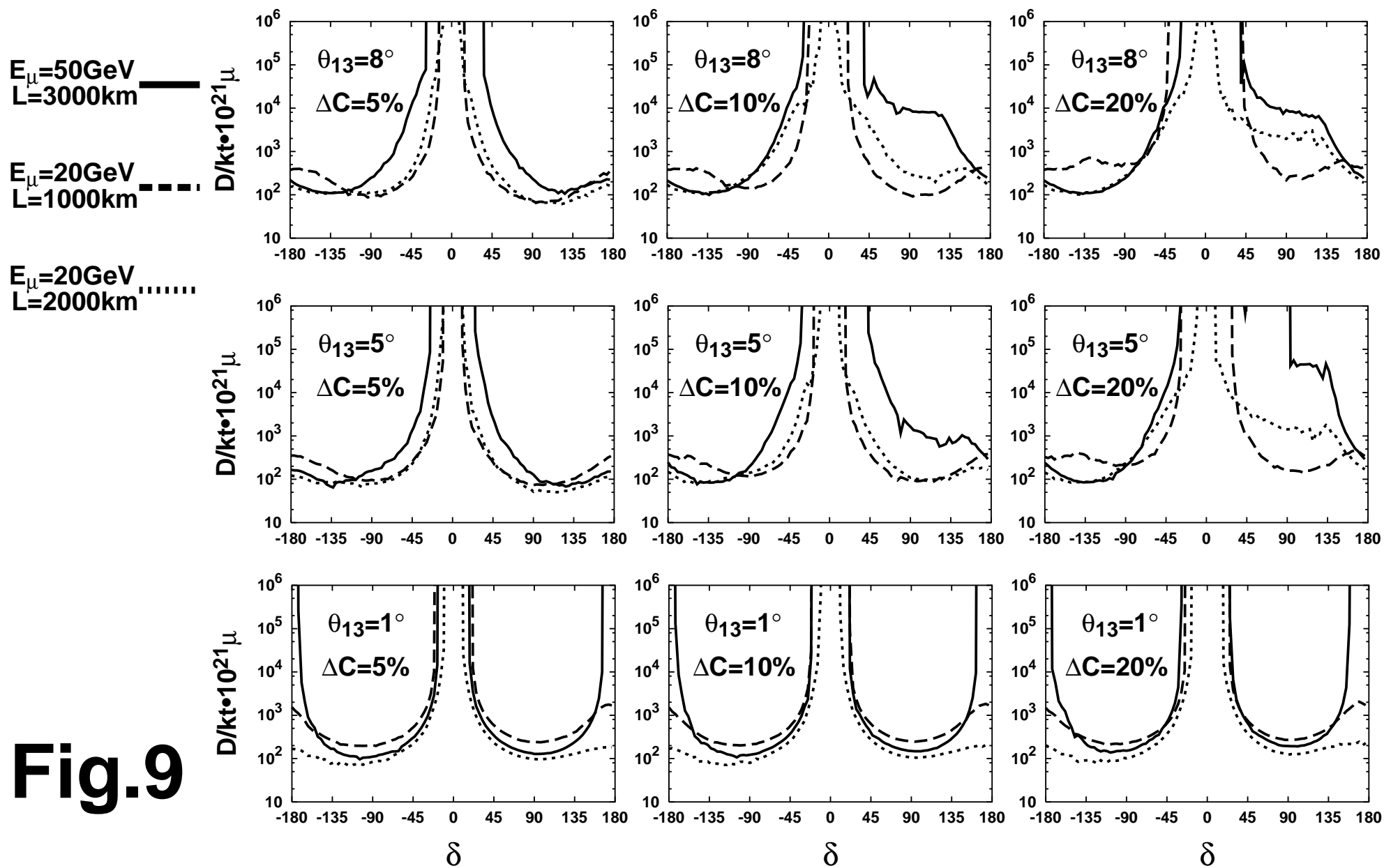
68%CL —
 90%CL - -
 99%CL

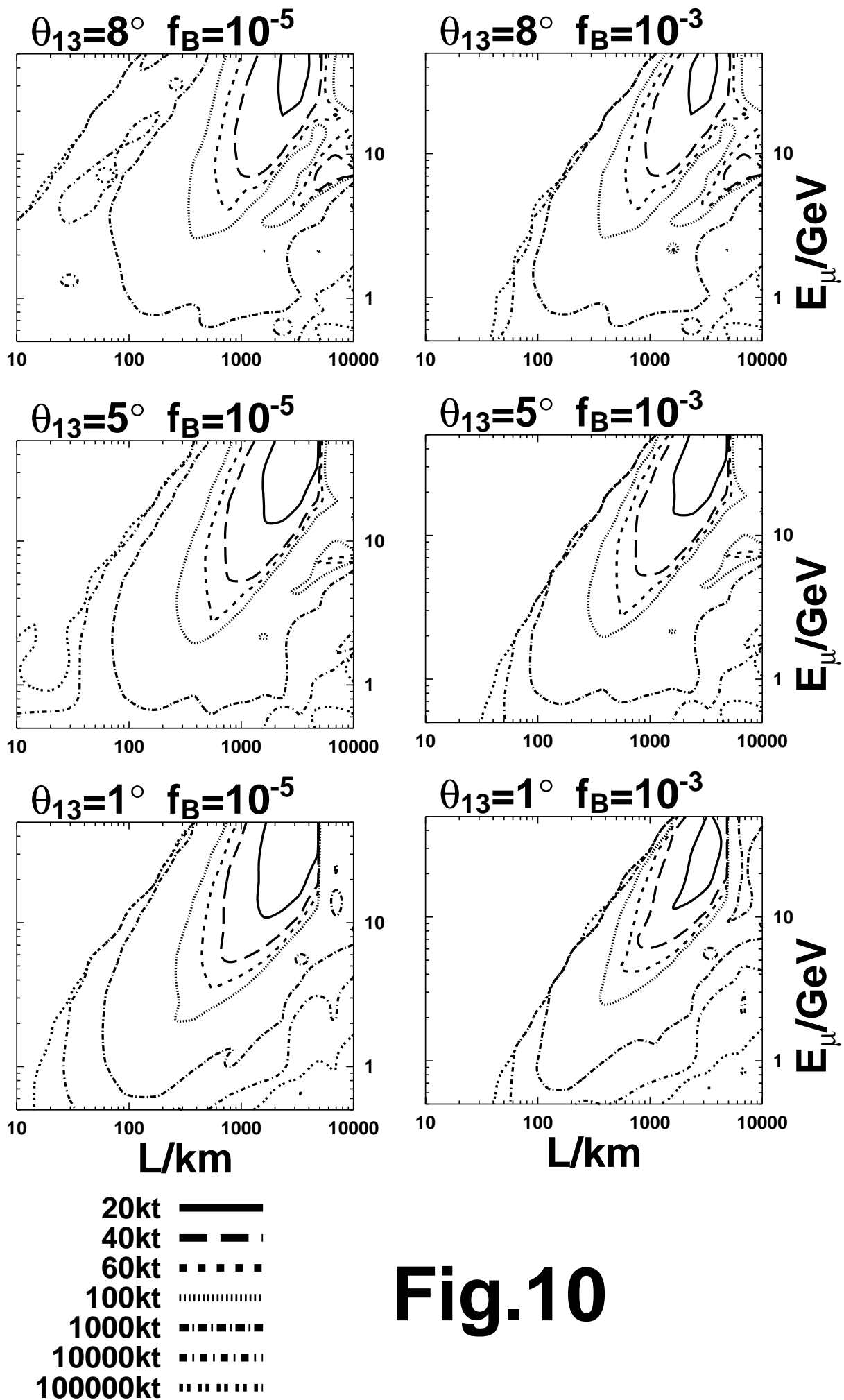
Fig.6

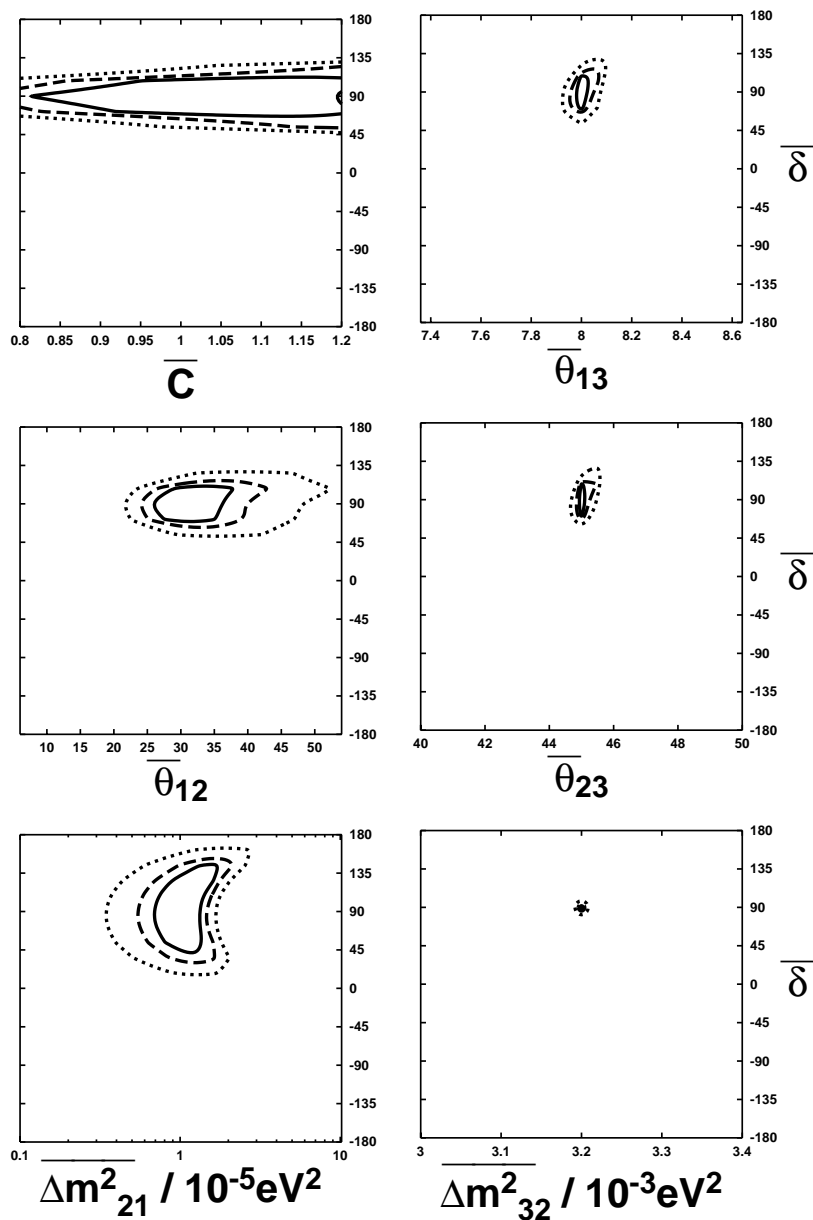


100kt
 1000kt - - - - -
 10000kt - . - . -
 100000kt

Fig.8







68%CL ---
 90%CL --- --
 99%CL

Fig.11

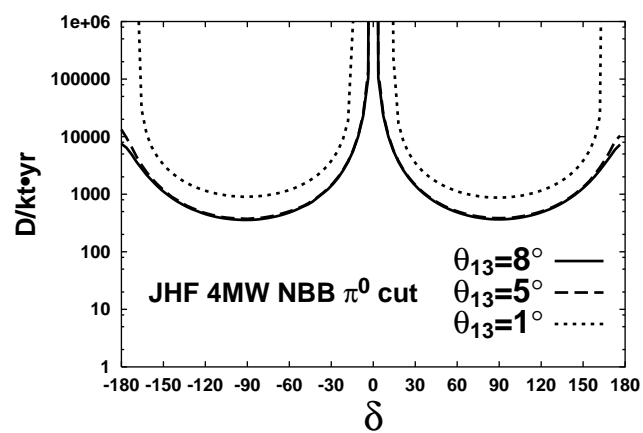
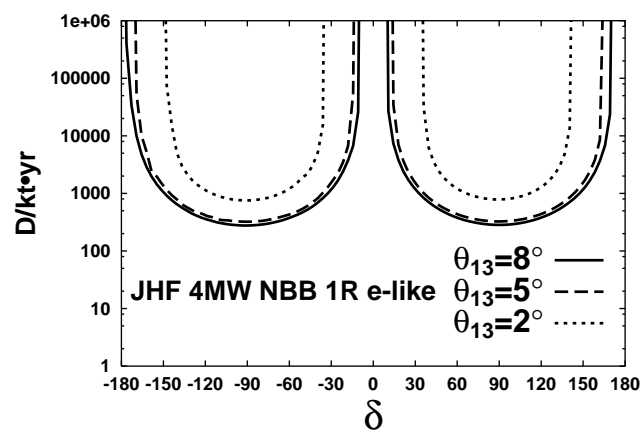


Fig.12